The distonic ion ·CH2CH2CH+OH, keto ion CH3CH2CH=O +·, enol ion CH3CH=CHOH+·, and related C3H6O+· radical cations. Stabilities and isomerization proclivities studied by dissociatio…

ARTICLE *in* JOURNAL OF THE AMERICAN SOCIETY FOR MASS SPECTROMETRY · JUNE 1996

Impact Factor: 2.95 · DOI: 10.1016/1044-0305(96)00053-0 · Source: PubMed

2 AUTHORS:

Michael J Polce
Independent Researcher
54 PUBLICATIONS **1,035** CITATIONS
SEE PROFILE

Chrys Wesdemiotis
University of Akron
259 PUBLICATIONS **5,720** CITATIONS
SEE PROFILE

The Distonic Ion $^{\cdot}CH_2CH_2CH^{+}OH$, Keto Ion $CH_3CH_2CH{=}O^{+\cdot}$, Enol Ion $CH_3CH{=}CHOH^{+\cdot}$, and Related $C_3H_6O^{+\cdot}$ Radical Cations. Stabilities and Isomerization Proclivities Studied by Dissociation and Neutralization–Reionization

Michael J. Polce and Chrys Wesdemiotis
Department of Chemistry, The University of Akron, Akron, Ohio, USA

Metastable ion decompositions, collision-activated dissociation (CAD), and neutralization–reionization mass spectrometry are utilized to study the unimolecular chemistry of distonic ion $^{\cdot}CH_2CH_2CH^{-}OH$ ($\mathbf{2}^{+\cdot}$) and its enol–keto tautomers $CH_3CH{=}CHOH^{+\cdot}$ ($\mathbf{1}^{+\cdot}$) and $CH_3CH_2CH{=}O^{+\cdot}$ ($\mathbf{3}^{+\cdot}$). The major fragmentation of metastable $\mathbf{1}^{+\cdot}$–$\mathbf{3}^{+\cdot}$ is $H^{\cdot}$ loss to yield the propanoyl cation, $CH_3CH_2C{\equiv}O^{+}$. This reaction remains dominant upon collisional activation, although now some isomeric $CH_2{=}CH{-}CH^{+}OH$ is coproduced from all three precursors. The CAD and neutralization–reionization ($^{+}NR^{+}$) spectra of keto ion $\mathbf{3}^{+\cdot}$ are substantially different from those of tautomers $\mathbf{2}^{+\cdot}$ and $\mathbf{1}^{+\cdot}$. Hence, $\mathbf{3}^{+\cdot}$ without sufficient energy for decomposition (i.e., "stable" $\mathbf{3}^{+\cdot}$) does not isomerize to the thermodynamically more stable ions $\mathbf{2}^{+\cdot}$ or $\mathbf{1}^{+\cdot}$, and the 1,4-H rearrangement $H{-}CH_2CH_2C\dot{H}{=}O^{+\cdot}$ ($\mathbf{3}^{+\cdot}$) → $^{\cdot}CH_2CH_2CH^{+}O{-}H$ ($\mathbf{2}^{+\cdot}$) must require an appreciable critical energy. Although the fragment ion abundances in the $^{+}NR^{+}$ (and CAD) spectra of $\mathbf{1}^{+\cdot}$ and $\mathbf{2}^{+\cdot}$ are similar, the relative and absolute intensities of the survivor ions (recovered $C_3H_6O^{+\cdot}$ ions in the $^{+}NR^{+}$ spectra) are markedly distinct and independent of the internal energy of $\mathbf{1}^{+\cdot}$ and $\mathbf{2}^{+\cdot}$. Furthermore, $\mathbf{1}^{+\cdot}$ and $\mathbf{2}^{+\cdot}$ show different MI spectra. Based on these data, distonic ion $\mathbf{2}^{+\cdot}$ does not spontaneously rearrange to enol ion $\mathbf{1}^{+\cdot}$ (which is the most stable $C_3H_6O^{+\cdot}$ of CCCO connectivity) and, therefore, is separated from it by an appreciable barrier. In contrast, the molecular ions of cyclopropanol ($\mathbf{4}^{+\cdot}$) and allyl alcohol ($\mathbf{5}^{+\cdot}$) isomerize readily to $\mathbf{2}^{+\cdot}$, via ring opening and 1,2-H^{-} shift, respectively. The sample found to generate the purest $\mathbf{2}^{+\cdot}$ is α-hydroxy-γ-butyrolactone. Several other precursors that would yield $\mathbf{2}^{+\cdot}$ by a least-motion reaction cogenerate detectable quantities of enol ion $\mathbf{1}^{+\cdot}$, or the enol ion of acetone ($CH_2{=}C(CH_3)OH^{+\cdot}$, $\mathbf{6}^{+\cdot}$), or methyl vinyl ether ion ($CH_3OCH{=}CH_2^{+\cdot}$, $\mathbf{7}^{+\cdot}$). Ion $\mathbf{6}^{+\cdot}$ is coproduced from samples that contain the $-CH_2-CH(OH)-CH_2-$ substructure, whereas $\mathbf{7}^{+\cdot}$ is coproduced from compounds with methoxy substituents. Compared to CAD, metastable ion characteristics combined with neutralization–reionization allow for a superior differentiation of the ions studied. *(J Am Soc Mass Spectrom 1996, 7, 573–589)*

Radical cations $C_3H_6O^{+\cdot}$ with the CCCO frame appear in the mass spectra of many organic compounds [1] and, therefore, have been investigated extensively both theoretically [2–6] and experimentally [7–14]. It is now established that enol ion $CH_3CH{=}CHOH^{+\cdot}$ ($\mathbf{1}^{+\cdot}$) is the most stable isomer of CCCO connectivity [15] and that the threshold dissociation of this cation yields the propanoyl ion, $CH_3CH_2C{\equiv}O^{+}$, by $H^{\cdot}$ loss [9–12]. Computational studies have shown that the lowest energy path for this fragmentation proceeds by an enol to keto tautomerization via the β-distonic ion $^{\cdot}CH_2CH_2CH^{+}OH$ ($\mathbf{2}^{+\cdot}$), namely, eq 1 [5, 6].

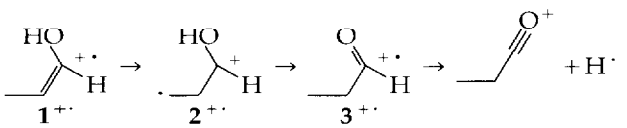

(1)

Address reprint requests to Dr. Chrys Wesdemiotis, Department of Chemistry, The University of Akron, Akron, OH 44325-3601.

1044-0305/96/$15.00
PII S1044-0305(96)00053-0

Received November 9, 1995
Revised January 11, 1996
Accepted February 2, 1996

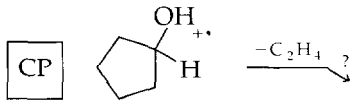

(2)

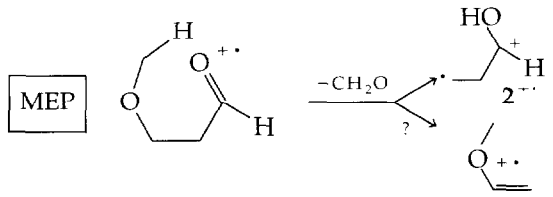

(3a)

(3b)

According to theory, distonic ion $\mathbf{2}^{+\cdot}$ is a distinct, bound species that resides in a deep potential energy well and is thermodynamically more stable than the keto ion $\mathbf{3}^{+\cdot}$ [5, 6]. Although often postulated to arise upon the rearrangement fragmentation of molecular cations that contain the C_3H_6O substructure [7–10, 12–14, 16], $\mathbf{2}^{+\cdot}$ has not been thoroughly characterized yet and, considering the attention devoted to similar distonic ions [17–19], direct experimental data on this cation are scarce. McAdoo and Hudson [9, 10] first proposed that $\mathbf{2}^{+\cdot}$ may be formed upon the dissociative ionization of cycloalkanols (eq 2) [9], possibly together with $\mathbf{1}^{+\cdot}$ and/or the enol ion of acetone [10]. These authors later reported that the $C_3H_6O^{+\cdot}$ ion generated by $CH_2{=}O$ elimination from ionized 3-methoxypropanal (eq 3a) most likely is $\mathbf{2}^{+\cdot}$; the corresponding collision-activated dissociation (CAD) spectrum was very similar to that of enol ion $\mathbf{1}^{+\cdot}$, but included a unique feature, namely, a more abundant m/z 43 fragment ($^{\cdot}CH_3$ loss) [12]. Unfortunately, such a fragment is not characteristic for structure $\mathbf{2}^{+\cdot}$ which bears no methyl substituent. The appearance energy of the $C_3H_6O^{+\cdot}$ ion from reaction 3a, determined by photoionization [12], led to a heat of formation of 757 kJ mol^{-1}. This value matches well the value for $\mathbf{2}^{+\cdot}$ theoretically predicted by the same authors (760 kJ mol^{-1}) [6], but also is very similar to the ΔH_f° of the isomeric methyl vinyl ether ion (761 kJ mol^{-1}) [15a] that can be accessed from the 3-methoxypropanal precursor (eq 3b). In fact, an admixture of the latter ion, which is known to lose $^{\cdot}CH_3$ upon collisional activation [20, 21], would explain the aforementioned increased intensity of m/z 43 in the CAD spectrum of $\mathbf{2}^{+\cdot}$. Most recently, Gu and Turecek [13] suggested that $\mathbf{2}^{+\cdot}$ is produced from ionized cis and trans 4-methylcyclohexanol, albeit contaminated with varying amounts of enol ion $\mathbf{1}^{+\cdot}$ and the isobaric $C_4H_{10}^{+\cdot}$ cation. In light of the confusing and limited information available about distonic ion $\mathbf{2}^{+\cdot}$ and its importance in the decomposition of other $C_3H_6O^{+\cdot}$ ions with the CCCO frame, we present here a detailed study of the unimolecular chemistry of $\mathbf{2}^{+\cdot}$. (Preliminary results of this study were presented at the 1993 and 1994 ASMS conferences [22].) The stability and fragmentations of $\mathbf{2}^{+\cdot}$ are probed by metastable ion (MI) and collision-activated dissociation [23] as well as by neutralization–reionization mass spectrometry (NRMS) [24–26].

Four relevant issues are addressed in this paper.

1. The isomerization extent of the molecular ion of propanal ($\mathbf{3}^{+\cdot}$) to the more stable distonic ion $\mathbf{2}^{+\cdot}$ is appraised. Many similar keto ions have been found to completely or extensively rearrange to more stable distonic isomers [27–29].
2. The composition of $C_3H_6O^{+\cdot}$ from more than 10 linear and cyclic compounds is examined to determine which structural features favor the production of distonic ion $\mathbf{2}^{+\cdot}$, and which favor the production of enol ion $\mathbf{1}^{+\cdot}$ or other pertinent $C_3H_6O^{+\cdot}$ isomers.
3. The relationship is determined between $\mathbf{2}^{+\cdot}$ and the molecular ions of cyclopropanol ($\mathbf{4}^{+\cdot}$) and allyl alcohol ($\mathbf{5}^{+\cdot}$), which represent the ring-closed and a tautomeric form of $\mathbf{2}^{+\cdot}$, respectively [22a]. Ions $\mathbf{4}^{+\cdot}$ and $\mathbf{5}^{+\cdot}$ have been studied previously [7, 11, 30–33], although mostly not together and never in conjunction with isomer $\mathbf{2}^{+\cdot}$. Photoionization breakdown experiments found $\mathbf{4}^{+\cdot}$ and $\mathbf{5}^{+\cdot}$ to be indistinguishable [32], whereas their CAD spectra were shown to be very similar to those of enol ion $\mathbf{1}^{+\cdot}$, which suggests equilibration to the enol ion [31].
4. Finally, this investigation briefly questions the stability of neutralized $\mathbf{2}^{+\cdot}$, that is, of the elusive 1,3-diradical $^{\cdot}CH_2CH_2CH^{\cdot}OH$, which has been implicated as an intermediate in the pyrolysis and photolysis of C_3H_6O and homologous compounds [34, 35].

Experimental

All experiments were conducted with a modified VG AutoSpec tandem mass spectrometer (VG Analytical Ltd., Manchester, UK) that has been described in detail previously [27]. This trisector E_1BE_2 instrument has one collision cell (Cls-1) in the field-free region following the ion source (FFR-1) and two more collision cells (Cls-2 and Cls-3), with an intermediate deflector, in the region between E_1B and E_2 (FFR-3). Tandem mass spectra (MI, CAD, or NRMS type) of source-generated precursor ions were acquired in FFR-3 by using E_1B as MS-1 and the second electric sector as MS-2. The structures of selected products in the MI and CAD spectra were further probed by MS^3 [23], where the fragment under investigation was formed in FFR-1 (via spontaneous or collision-activated decomposition of the $C_3H_6O^{+\cdot}$ precursor) and then transmitted through appropriate setting of E_1B to FFR-3 for the acquisition of its own CAD spectrum.

CAD spectra were measured by using O_2 as the collision target (in Cls-3). Neutralization–reionization ($^+NR^+$) mass spectra [24–26] were acquired by neutralization of the $C_3H_6O^{+\cdot}$ precursor ion in Cls-2 with Xe and reionization of the emerging neutrals to cations in Cls-3 with O_2. Neutral fragment–reionization ($^+N_fR^+$) spectra [36] were obtained similarly by replacing the neutralization target (Xe) with He, which,

owing to its poor neutralization efficiency, mainly causes CAD, not charge exchange of the precursor ion [37]. Note, that CAD liberates many neutral fragments simultaneously and that the $^+N_fR^+$ spectrum observed represents the convolution of the collision-induced dissociative ionization (CIDI) spectra [38] of the individual neutral losses.

For $^+NR^+$ or $^+N_fR^+$, the pressure of each collision gas was adjusted to attenuate the precursor ion (main beam) by 20% (overall transmittance 64%). CAD was effected at 60% transmittance. The samples were ionized by electron impact (EI) at 70 eV (or as stated) and all ions that exited the ion source were accelerated to 8 keV. Kinetic energy releases were calculated from peak widths at half height ($T_{0.5}$) [39] and are corrected for the main beam width by using established procedures [40]. The $^+NR^+$ yield (i.e., absolute abundance) of the survivor ion or another $^+NR^+$ product was calculated by dividing its flux in the $^+NR^+$ spectrum by the flux of the unattenuated main beam. The spectra shown represent multiscan summations and the reproducibilities of relative and absolute abundances are better than plus or minus 10 and 30%, respectively.

For several of the samples investigated, the $C_3H_6O^{+\cdot}$ precursor (m/z 58) is contaminated by the ^{13}C satellite of $C_3H_5O^+$ (m/z 57). For example, the m/z 58 peak of allyl alcohol contains 8.5% $^{13}C^{12}C_2H_5O^+$. The MI, CAD, and $^+NR^+$ spectra of $C_3H_5O^+$ from allyl alcohol reveal however that, at such a proportion, ^{13}C satellites do not contribute appreciably to the MI, CAD, or $^+NR^+$ spectra of $C_3H_6O^{+\cdot}$. Specifically, based on the $^+NR^+$ yield of the survivor ion of $C_3H_5O^+$ from allyl alcohol, which is over 10 times smaller than that of the allyl alcohol ion itself, the survivor ion of allyl alcohol (m/z 58) contains much less than 8.5% $^{13}C^{12}C_2H_5O^+$. A few $C_3H_6O^{+\cdot}$ precursors contain admixtures of the isobaric hydrocarbon ions $C_4H_{10}^{+\cdot}$ and/or $^{13}C^{12}C_3H_9^+$; these impurities are readily detected by their abundant m/z 42 fragments in MI spectra as well as by the appearance of m/z 48–51 fragments ($C_4H_{0-3}^+$) in CAD and $^+NR^+$ spectra. The $^+NR^+$ yields of m/z 57 and 58 from $C_4H_{10}^{+\cdot}$ and $^{13}C^{12}C_3H_9^+$ are extremely low (again, more than 10 times smaller than those of m/z 57 and 58 from $C_3H_6O^{+\cdot}$); therefore, the hydrocarbon cations do not affect noticeably the [m/z 58]:[m/z 57] ratio, which was used to deduce the structure of $C_3H_6O^{+\cdot}$.

Cyclopropanol was synthesized from epichlorohydrin, magnesium bromide, ferric chloride, and ethylmagnesium bromide by the procedure of Cottle [41] as modified by Roberts and Chambers [42]. Methyl vinyl ether and 3-methoxypropan-1-ol were purchased from Matheson Gas Products (Secaucus, NJ) and Karl Industries Inc. (Aurora, OH), respectively. All other chemicals were acquired from Aldrich Chemical Co. (Milwaukee, WI). Cyclopropanol was purified by repeated distillation, whereas all other samples were introduced into the mass spectrometer as received from the manufacturer.

Results and Discussion

Unimolecular Chemistry of Enol Ion $CH_3CH{=}CHOH^{+\cdot}$ (1$^{+\cdot}$), Distonic Ion $^{\cdot}CH_2CH_2CH^+OH$ (2$^{+\cdot}$), and Keto Ion $CH_3CH_2CH{=}O^{+\cdot}$ (3$^{+\cdot}$)

From the various potential precursors used for the synthesis of distonic ion **2**$^{+\cdot}$ in this study, only α-hydroxy-γ-butyrolactone (HBL) produces this ion with an adequate intensity and essentially pure from isomeric and isobaric contaminants (vide infra). Dissociative EI of this compound leads to the incipient $^{\cdot}CH_2CH_2CH^+OH$ via ring opening and elimination of a small stable molecule (eq 4), that is, a reaction sequence that is commonly encountered in the preparation of gaseous distonic ions [18, 19, 21, 43]. First, the unimolecular reactivity of **2**$^{+\cdot}$ (from HBL, eq 4) is compared to those of its well known enol–keto tautomers **1**$^{+\cdot}$ and **3**$^{+\cdot}$ [7, 11, 44]. The two latter radical cations are formed by the McLafferty rearrangement of 2-methylpentanal (eq 5) and direct ionization of propanal, respectively.

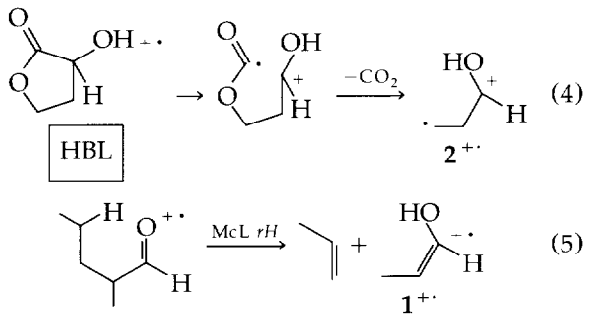

(4)

(5)

Metastable Ion Dissociations and Their Importance After Collisional Activation. Metastable **2**$^{+\cdot}$ that decomposes in FFR-3 has an average lifetime of 10.5 μs and primarily loses H$^{\cdot}$ to form $C_3H_5O^+$ (m/z 57), see Table 1. For isomers **1**$^{+\cdot}$ and **3**$^{+\cdot}$, H$^{\cdot}$ elimination is the only reaction that takes place in this time window, whereas **2**$^{+\cdot}$ undergoes an additional, minor dissociation that produces m/z 30 (Figure 1). MS/MS/MS on the $C_3H_5O^+$ fragment formed from metastable **1**$^{+\cdot}$–**3**$^{+\cdot}$ in FFR-1 shows that it basically is the propanoyl cation $CH_3CH_2C{\equiv}O^+$ in all three cases (Figure 2), in line with the previous findings of McAdoo and co-workers [9, 12] and the theoretical prediction that CCCO-framed $C_3H_6O^{+\cdot}$ ions with threshold energies isomerize to propanal ions before H-atom cleavage (eq 1) [5, 6]. The latter mechanism is consistent with earlier reported labeling studies, based on which keto ion **3**$^{+\cdot}$ only loses the carbonyl-bonded hydrogen [31], whereas enolic **1**$^{+\cdot}$ and distonic **2**$^{+\cdot}$ (from 3-methoxypropanal [12]) mainly (> 90%) eliminate one of their carbon-bonded H-atoms [9, 11, 12, 17, 30, 31].

The m/z 57 signals from all three precursors have the same gaussian peak shape (Figure 1) and the corre-

Table 1. MI spectra of $C_3H_6O^{+\cdot}$ isomers

Precursor	Mass-to-charge ratio[a]				Assigned structure
	30[b]	42[c]	43	57[d]	
2-Methylpentanal				100	$\mathbf{1}^{+\cdot}$
α-Hydroxy-γ-butyrolactone (HBL)	1.2 (ng)			100	$\mathbf{2}^{+\cdot}$
Propanal				100	$\mathbf{3}^{+\cdot}$
Methoxyacetone			100 (g)		$\mathbf{6}^{+\cdot}$
Methyl vinyl ether			100 (ng)		$\mathbf{7}^{+\cdot}$
Cyclopentanol (CP)	0.29 (ng)		2.2 (g)	100	$\mathbf{2}^{+\cdot}$ & $\mathbf{6}^{+\cdot}$[e]
3-Methoxypropanal (MEP)	0.41[f]		5.7 (ng)	100	$\mathbf{2}^{+\cdot}$ & $\mathbf{7}^{+\cdot}$[e]
4-Methylcyclohexanol (MCH)	0.38[f]	2.5	[f] (g)	100	$\mathbf{1}^{+\cdot}$ & $\mathbf{2}^{+\cdot}$ & $\mathbf{6}^{+\cdot}$
3-Hydroxytetrahydrofuran (HTF)	0.61 (ng)		0.67 (g)	100	$\mathbf{2}^{+\cdot}$ & $\mathbf{6}^{+\cdot}$
3-Methoxypropan-1-ol (MP)	0.51[f]		1.2 (ng)	100	$\mathbf{2}^{+\cdot}$ & $\mathbf{7}^{+\cdot}$
2-Methylbutanal		11		100	$\mathbf{1}^{+\cdot}$
2-Methylundecanal		1.2		100	$\mathbf{1}^{+\cdot}$
Pentanal		9.8		100	$\mathbf{1}^{+\cdot}$
Hexanal		8.5		100	$\mathbf{1}^{+\cdot}$
Cyclopropanol	0.33 (g)		0.15 (g)	100	$\mathbf{2}^{+\cdot}$ & $\mathbf{6}^{+\cdot}$
Allyl alcohol	0.16 (g)			100	$\mathbf{2}^{+\cdot}$

[a] Relative abundances in percent of base peak (from peak areas).
[b] The letters "ng" and "g" in parentheses designate a nongaussian or gaussian peak shape, respectively.
[c] This fragment ($C_3H_6^{+\cdot}$) is due to isobaric $C_4H_{10}^{+\cdot}$.
[d] Gaussian signal for all precursors.
[e] Some $\mathbf{1}^{+\cdot}$ also could be present; see text.
[f] Weak intensity, collisional background, and/or adjacent artefact peaks make it impossible to determine the peak shape and/or its abundance.

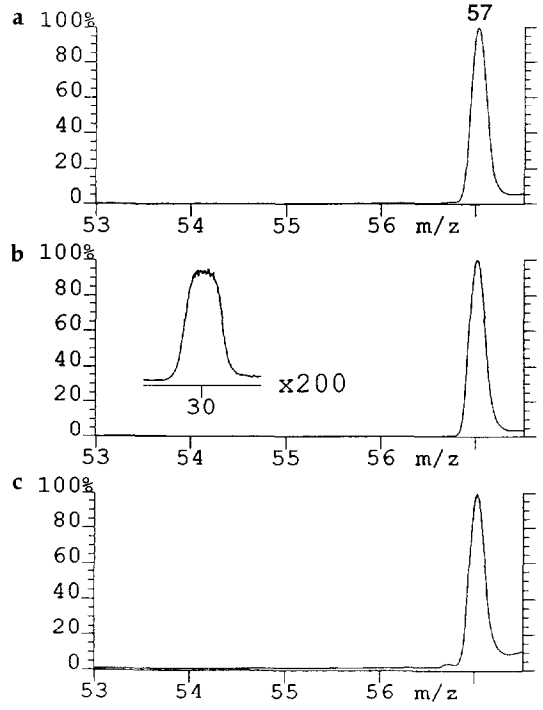

Figure 1. MI spectra of (**a**) enol ion $CH_3CH{=}CHOH^{+\cdot}$ ($\mathbf{1}^{+\cdot}$; from 2-methylpentanal, eq 5), (**b**) distonic ion $^{\cdot}CH_2CH_2CH^{+}OH$ ($\mathbf{2}^{+\cdot}$; from α-hydroxy-γ-butyrolactone, eq 4), and (**c**) keto ion $CH_3CH_2CH{=}O^{+\cdot}$ ($\mathbf{3}^{+\cdot}$; from propanal). Unimolecular dissociation takes place in FFR-3. There is no m/z 30 peak above collisional background in the spectra of $\mathbf{1}^{+\cdot}$ and $\mathbf{3}^{+\cdot}$.

sponding kinetic energy releases are very similar ($T_{0.5} \approx 200$ meV). Our $T_{0.5}$ values are in good agreement with those reported for tautomers $\mathbf{1}^{+\cdot}$ and $\mathbf{3}^{+\cdot}$ by Holmes et al. [31], Hoppilliard et al. [3], and Turecek et al. [11]. The large kinetic energy releases observed upon $CH_3CH_2C{\equiv}O^{+}$ formation from $\mathbf{1}^{+\cdot}$–$\mathbf{3}^{+\cdot}$ indicate that there is a significant reverse activation energy for this reaction. For precursors $\mathbf{1}^{+\cdot}$ and $\mathbf{2}^{+\cdot}$, which must first rearrange to yield the propanoyl fragment (eq 1), a large $T_{0.5}$ is not unusual [23, 39, 40, 45]. The large $T_{0.5}$ value for the propanal ion, from which $H^{\cdot}$ is lost by a direct bond cleavage (see preceding paragraph [31]), is however surprising. Evidently, the reaction $\mathbf{3}^{+\cdot} \rightarrow CH_3CH_2C{\equiv}O^{+} + H^{\cdot}$ is not continuously endothermic and has a sizable reverse barrier. The same conclusion was reached earlier by Turecek et al. [11] and is in accord with preliminary ab initio computations by Bouchoux [Bouchoux, G., private communication; ab initio calculations at the MP2/6-31*//HF/6-31G*/ZPE level find the reaction $CH_3CH_2CH{=}O^{+\cdot} \rightarrow CH_3CH_2CO^{+} + H^{\cdot}$ to have a reverse activation energy of 30 ± 10 kJ mol^{-1}. This theoretical study, which updates ref 5, also provides new values for the heat of formation of distonic ion $^{\cdot}CH_2CH_2CH^{+}OH$ and for several isomerization barriers relevant to this ion, which include those that separate it from tautomers $CH_3CH_2CH{=}O^{+\cdot}$ and $CH_3CH{=}CHOH^{+\cdot}$, as well as those needed for cyclopropanol and allyl alcohol ions to rearrange to $^{\cdot}CH_2CH_2CH^{+}OH$ (see Figure 3 or text for the exact

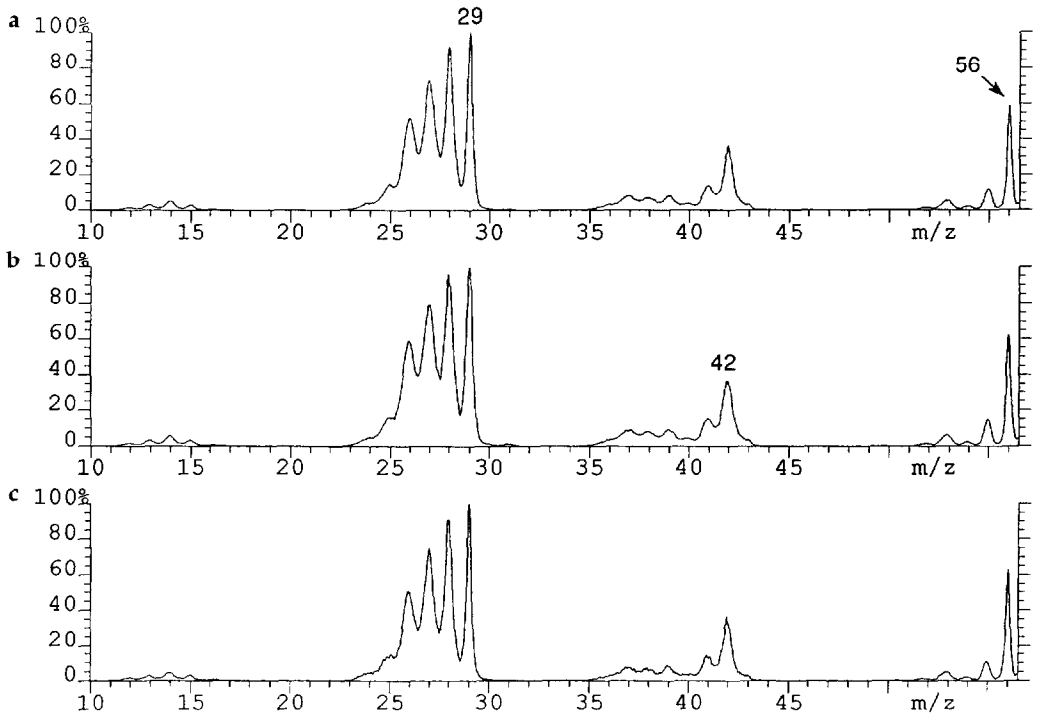

Figure 2. MS/MS/MS spectra (acquired in FFR-3) of $C_3H_5O^+$ produced in FFR-1 from metastable (a) $CH_3CH{=}CHOH^{+\cdot}$ ($\mathbf{1}^{+\cdot}$), (b) $^{\cdot}CH_2CH_2CH^+OH$ ($\mathbf{2}^{+\cdot}$), and (c) $CH_3CH_2CH{=}O^{+\cdot}$ ($\mathbf{3}^{+\cdot}$). $C_3H_5O^+$ from metastable $\mathbf{3}^{+\cdot}$, which has the propanoyl structure [9, 12], provides a reference spectrum for the $CH_3CH_2C{\equiv}O^+$ cation.

values).] All these results are reconciled by the potential energy diagram illustrated in Figure 3.

The elimination of $H^{\cdot}$ remains the major decomposition channel of $\mathbf{1}^{+\cdot}$–$\mathbf{3}^{+\cdot}$ even after CAD (Figure 4). However now, the MS/MS/MS spectrum of the emerging $C_3H_5O^+$ product (Figure 5a) contains more m/z 31, 36–39, and 55 than the spectrum of propanoyl (Figure 2c). These extra fragments are indicative of the isomeric 1-hydroxy-2-propenium cation $CH_2{=}CHCH^+OH$ (protonated acrolein); compare Figure 5b [46]. It is noteworthy that $CH_2{=}CHCH^+OH$ is observed not only from enolic $\mathbf{1}^{+\cdot}$ and distonic $\mathbf{2}^{+\cdot}$, which can yield this carbenium ion by direct cleavages of an H-atom, but also from keto ion $\mathbf{3}^{+\cdot}$, which must undergo prior H rearrangement. Such behavior attests that collisionally activated $\mathbf{1}^{+\cdot}$–$\mathbf{3}^{+\cdot}$ can readily interconvert before unimolecular decomposition. In contrast to collisionally excited $\mathbf{1}^{+\cdot}$–$\mathbf{3}^{+\cdot}$, metastable $\mathbf{1}^{+\cdot}$–$\mathbf{3}^{+\cdot}$ produce barely any $CH_2{=}CHCH^+OH$ as shown, for example, by the negligible abundance of m/z 31 in the MS/MS/MS spectra of Figure 2. Hence, the appearance energy of the $CH_2{=}CHCH^+OH$ fragment must be larger than that of the propanoyl fragment (cf. Figure 3).

As previously mentioned, a minor dissociation of metastable $\mathbf{2}^{+\cdot}$ gives rise to a fragment of m/z 30; the corresponding peak shape is nongaussian, with $T_{0.5}$ = 84 meV (Figure 1b). The MS/MS/MS spectrum of m/z 30 (Figure 6) indicates the composition $C_2H_6^{+\cdot}$ (CO loss). The $C_2H_6^{+\cdot}$ fragment is unique for $\mathbf{2}^{+\cdot}$ (Table 1); nevertheless it does not diagnose any specific structural element in the distonic ion $^{\cdot}CH_2CH_2CH^+OH$. If collision gas is slowly admitted in FFR-3, the peak shape of m/z 30 gradually changes to gaussian (cf. Figure 1b versus Figure 4b). When the collision gas is introduced in FFR-1, two signals appear at m/z 30, namely, approximately 10% $[C, H_2, O]^{+\cdot}$ and approximately 90% $C_2H_6^{+\cdot}$ (separable owing to the superior product ion resolution of linked scanning [23]). The MS/MS/MS spectrum of the combined m/z 30 peak remains similar to Figure 6. Apparently, the amount of $[C, H_2, O]^{+\cdot}$ formed is too small to produce visible fragments at m/z 16–18, which would allow one to determine the structure of this fragment ($CHOH^{+\cdot}$ or $CH_2{=}O^{+\cdot}$) [16, 47]. The simplest dissociation route to $[C, H_2, O]^{+\cdot}$ proceeds via the direct cleavage

$$^{\cdot}CH_2CH_2CH^+OH\,(\mathbf{2}^{+\cdot}) \rightarrow CH_2{=}CH_2 + CHOH^{+\cdot}$$

and leads to the carbenic isomer. The coproduction of approximately 10% $[C, H_2, O]^{+\cdot}$ cannot be solely responsible for the complete change of the peak shape of m/z 30 upon admission of collision gas in FFR-3. Most probably, collisional activation also opens a new pathway(s) to the major $C_2H_6^{+\cdot}$ component, that mechanistically differ from the pathway taking place at threshold [40, 45].

The critical energies required to form $CH_3CH_2C{\equiv}O^+$ (m/z 57) and $C_2H_6^{+\cdot}$ (m/z 30) differ

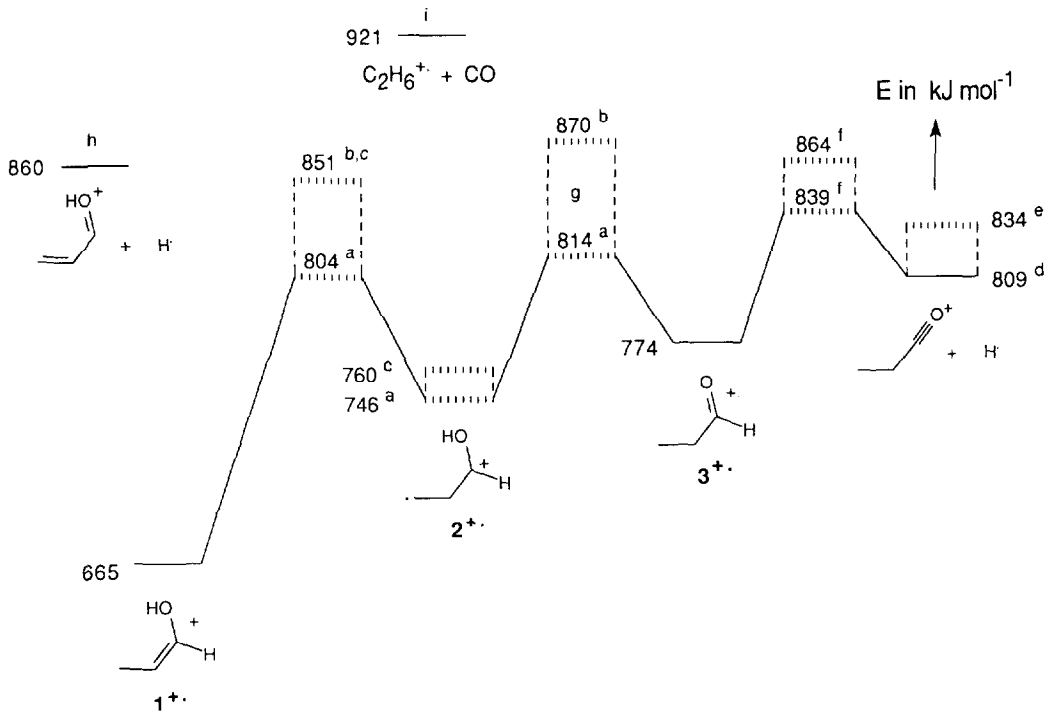

Figure 3. Potential energy diagram for the reactions of metastable $\mathbf{1}^{+\cdot}$–$\mathbf{3}^{+\cdot}$. Solid lines designate experimental data and broken lines designate theoretical data. Unless noted otherwise, heats of formation are from ref 15. [a]Bouchoux, G., private communication. [b]Reference 5. [c]Reference 12. [d]Based on $\Delta H_f^\circ(CH_3CH_2C{\equiv}O^+) = 591$ kJ mol^{-1} (Traeger, J. C. *Org. Mass Spectrom.* **1985**, *20*, 223–227). [e]Using $\Delta H_f^\circ(CH_3CH_2C{\equiv}O^+) = 616$ kJ mol^{-1}, predicted by ab initio computations at the G2 level (Scott, A. P.; Radom, L., private communication). [f]Obtained by adding to $\Sigma\Delta H_f^\circ(CH_3CH_2C{\equiv}O^+ + {}^{\cdot}H)$ the reverse activation energy calculated by Bouchoux (private communication). The presence of such a reverse barrier is revealed by this and other [3, 11, 31] studies. [g]According to the predicted transition state levels shown in this diagram, the dissociations $\mathbf{1}^{+\cdot} \rightarrow C_3H_5O^+$ and $\mathbf{2}^{+\cdot} \rightarrow C_3H_5O^+$ require the same critical energy (because $\mathbf{1}^{+\cdot} \rightarrow \mathbf{2}^{+\cdot}$ costs less energy than $\mathbf{2}^{+\cdot} \rightarrow \mathbf{3}^{+\cdot}$). Experimentally (from appearance energies), the transition state energies of the latter two reactions are indeed found to be similar; they lie at 854 [11] and 865 kJ mol^{-1} [12], respectively. [h]The transition state for $\mathbf{1}^{+\cdot} \rightarrow CH_2{=}CHCH^+OH + {}^{\cdot}H$ has been estimated to lie about 920 kJ mol^{-1} [11]. [i]The peak shape and $T_{0.5}$ value observed for this reaction (Figure 1b) point out that its transition state lies above 921 kJ mol^{-1}.

by over 50 kJ mol^{-1}, compare Figure 3. The much greater amount needed for the latter rearrangement explains the very small yield of ethane ion in the MI spectrum of $\mathbf{2}^{+\cdot}$ (Table 1). Metastable $\mathbf{1}^{+\cdot}$ and $\mathbf{3}^{+\cdot}$ reacting in FFR-3 form no detectable amount of m/z 30, even though they can interconvert to $\mathbf{2}^{+\cdot}$ at the energy level that leads to this fragment (Figure 3). Presumably, the overall process (i.e., isomerization of $\mathbf{1}^{+\cdot}$ or $\mathbf{3}^{+\cdot}$ to $\mathbf{2}^{+\cdot}$ and subsequent loss of CO) becomes too slow to produce an observable metastable signal. In addition, the population of $\mathbf{1}^{+\cdot}$ and $\mathbf{3}^{+\cdot}$ with sufficient internal energy for spontaneous dissociation to $C_2H_6^{+\cdot}$ + CO may be negligibly small. For ion $\mathbf{3}^{+\cdot}$, this assumption is verified by the photoelectron (PE) spectrum of propanal. PE spectra are believed to adequately describe the internal energy ranges deposited on EI [48]; that of propanal displays a large gap ($\sim$ 100 kJ mol^{-1}) about the energy necessary for $C_2H_6^{+\cdot}$ formation [49], explaining the lack of CO loss from $\mathbf{3}^{+\cdot}$. As expected, collisionally activated $\mathbf{1}^{+\cdot}$ and $\mathbf{3}^{+\cdot}$, which are supplied the missing excitation, do form fragments at m/z 30 (Figure 4). As with isomer $\mathbf{2}^{+\cdot}$, CAD of $\mathbf{1}^{+\cdot}$ and $\mathbf{3}^{+\cdot}$ generates mainly $C_2H_6^{+\cdot}$ plus some $[C, H_2, O]^{+\cdot}$. The parallel reactivity to m/z 30 of collisionally excited $\mathbf{1}^{+\cdot}$–$\mathbf{3}^{+\cdot}$ further documents the high propensity of these tautomers for dissociation through common intermediates.

Because metastable $\mathbf{2}^{+\cdot}$ *can* form $C_2H_6^{+\cdot}$, it should also be energetically capable of producing some $CH_2{=}CHCH^+OH$ (viz. Figure 3). This theory is corroborated by the MS/MS/MS spectra of metastably generated $C_3H_5O^+$ (Figure 2); the spectrum of $C_3H_5O^+$ from $\mathbf{2}^{+\cdot}$ (Figure 2b) contains a trace of m/z 31, which is diagnostic of $CH_2{=}CHCH^+OH$ (vide supra), thereby verifying the formation of a small amount of $CH_2{=}CHCH^+OH$ from precursor $\mathbf{2}^{+\cdot}$.

Theoretical data on the mechanism(s) of $C_2H_6^{+\cdot}$ formation from $\mathbf{1}^{+\cdot}$–$\mathbf{3}^{+\cdot}$ are not available. This fragment could arise via ion–molecule complexes, for example, through the sequence $^{\cdot}CH_2CH_2CH^+OH \rightarrow C_2H_4/CHOH^{+\cdot} \rightarrow C_2H_6^{+\cdot}/CO \rightarrow C_2H_6^{+\cdot} + CO$ [50]. Alternatively, $C_2H_6^{+\cdot}$ + CO may be formed after isomerization of the precursor ion to the carbenic species $CH_3CH_2{-}C{-}OH^{+\cdot}$ [5, 51]. A third possible path-

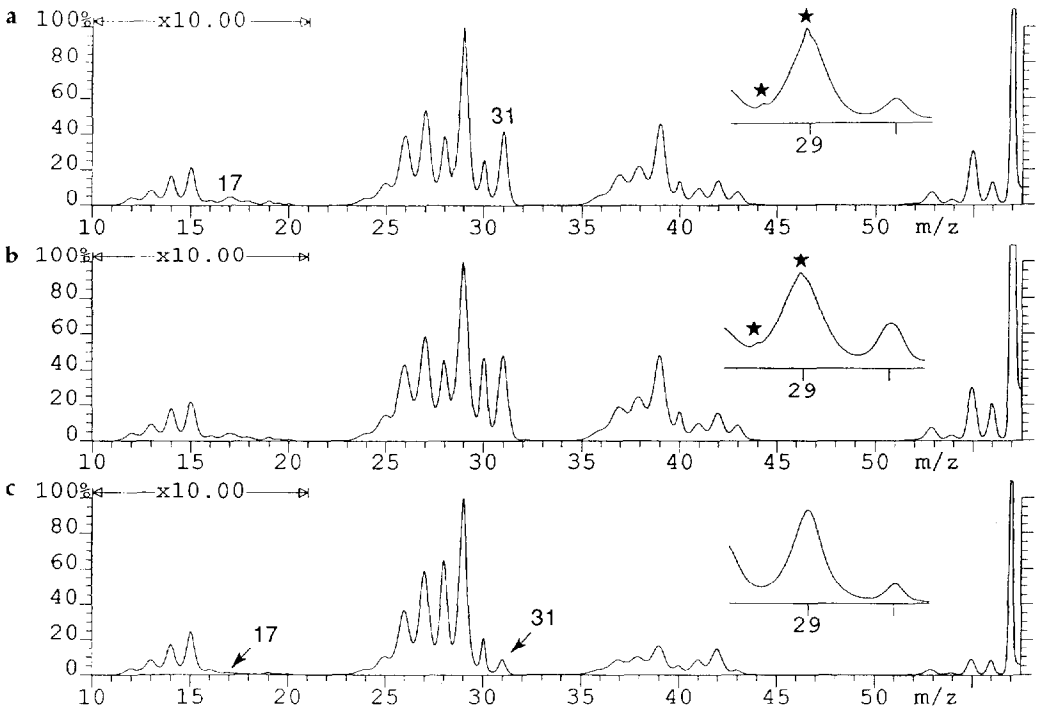

Figure 4. CAD spectra of (**a**) enol ion $CH_3CH{=}CHOH^{+\cdot}$ ($\mathbf{1}^{+\cdot}$), (**b**) distonic ion $^{\cdot}CH_2CH_2CH^{+}OH$ ($\mathbf{2}^{+\cdot}$), and (**c**) keto ion $CH_3CH_2CH{=}O^{+\cdot}$ ($\mathbf{3}^{+\cdot}$). Collisional activation takes place in FFR-3. Relative to [m/z 29], the abundance of m/z 57 is 170% in (a), 500% in (b) and 142% in (c). The m/z 29–30 region has been expanded in the insets to better show the presence of $C_3H_5O^{2+}$ and $C_3H_6O^{2+}$ dications (marked by *) in the spectra of $\mathbf{1}^{+\cdot}$ and $\mathbf{2}^{+\cdot}$.

way could involve the keto ion $CH_3CH_2CH{=}O^{+\cdot}$ as the reacting configuration for CO rupture.

Collision-Activated Dissociation. The CAD spectrum of $\mathbf{2}^{+\cdot}$ is practically superimposable on that of enol ion $\mathbf{1}^{+\cdot}$ (Figure 4). Only one minor difference is evident: the m/z 30 and 57 fragments are more abundant for $\mathbf{2}^{+\cdot}$. However, because m/z 30 and 57 also are present in the MI spectrum (vide supra), their relative intensities may be sensitive to internal energy effects and cannot be used for structural distinction. Compared to ions $\mathbf{1}^{+\cdot}$ and $\mathbf{2}^{+\cdot}$, keto isomer $\mathbf{3}^{+\cdot}$ gives rise to a unique

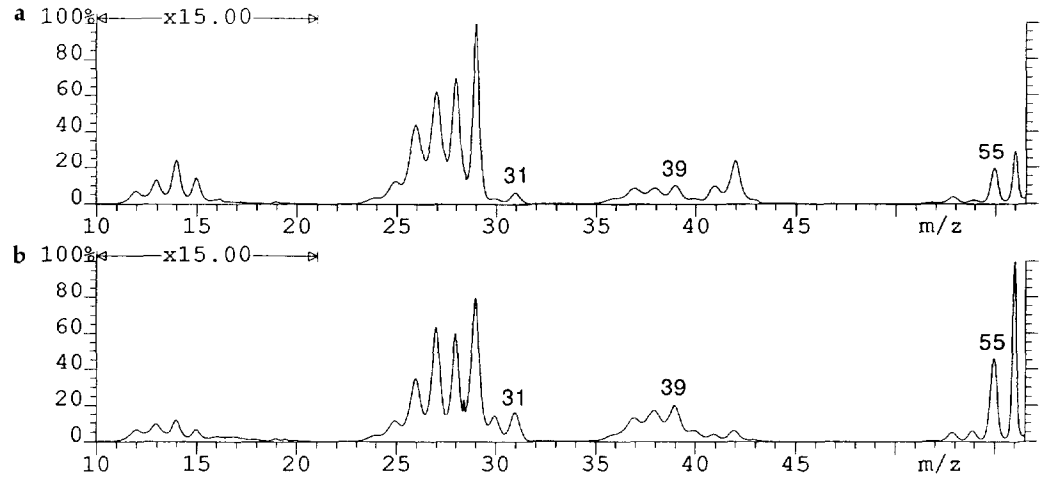

Figure 5. (**a**) MS/MS/MS spectrum (acquired in FFR-3) of $C_3H_5O^{+}$ produced in FFR-1 from collisionally activated $CH_3CH{=}CHOH^{+\cdot}$ ($\mathbf{1}^{+\cdot}$). Precursors $^{\cdot}CH_2CH_2CH^{+}OH$ ($\mathbf{2}^{+\cdot}$) and $CH_3CH_2CH{=}O^{+\cdot}$ ($\mathbf{3}^{+\cdot}$) give rise to quite similar spectra. (**b**) Reference CAD spectrum (MS/MS) of $CH_2{=}CH{-}CH^{+}OH$ formed in the ion source by self-protonation of acrolein ($CH_2{=}CH{-}CHO$).

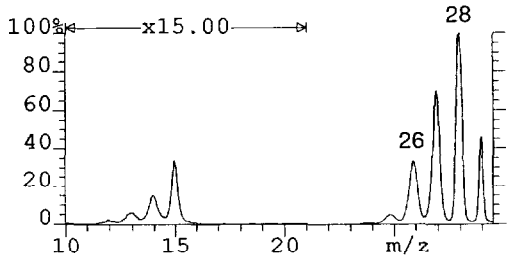

Figure 6. MS/MS/MS spectrum (acquired in FFR-3) of the m/z 30 fragment generated from metastable $^{\cdot}CH_2CH_2CH^+OH$ ($2^{+\cdot}$) in FFR-1.

and structurally indicative CAD spectrum. Note that m/z 31 ($^+CH_2OH$) and 17 (OH^+), which are characteristic for OH-bearing structures (such as $\mathbf{1}^{+\cdot}$ and $\mathbf{2}^{+\cdot}$) [48], are markedly smaller for the keto ion (Figure 4c). Moreover, there are no detectable charge stripping products in the CAD spectrum of $\mathbf{3}^{+\cdot}$. In sharp contrast, the enol and distonic ions, which can better support two separated charges [23], produce clearly visible $C_3H_6O^{2+}$ (m/z 29) and $C_3H_5O^{2+\cdot}$ (m/z 28.5) (viz. Figure 4a and b).

Neutral Fragment–Reionization. CIDI [25, 26, 38] of the neutral losses released from collisionally activated $\mathbf{1}^{+\cdot}$–$\mathbf{3}^{+\cdot}$ gives rise to the neutral fragment–reionization ($^+N_fR^+$) spectra of Figure 7. Helium was used for CAD of the mass-selected reactant ions (m/z 58). Due to its high ionization energy [15], this target minimizes the extent of concomitant charge exchange [37]. Still, some neutralization takes place, as shown by the appearance of a recovered, that is, neutralized–reionized, m/z 58 (Figure 7). This ion and the weak signals above m/z 29 are attributed to neutralization–reionization ($^+NR^+$) of $1^{+\cdot}$–$3^{+\cdot}$ (vide infra). On the other hand, the major source of $m/z \leq 29$ should be the neutral fragments eliminated upon CAD of $\mathbf{1}^{+\cdot}$–$\mathbf{3}^{+\cdot}$.

Enol ion $\mathbf{1}^{+\cdot}$ and distonic ion $\mathbf{2}^{+\cdot}$ yield the same fragment ions on CAD (viz. Figure 4a and b). It is, therefore, not surprising that the corresponding $^+N_fR^+$ spectra (i.e., the complementary neutral losses) also are essentially identical (Figure 7a and b). In contrast, the $^+N_fR^+$ spectrum of keto ion $\mathbf{3}^{+\cdot}$ (Figure 7c) is dominated by m/z 28 and displays several distinctive features, inter alia less abundant m/z 17–18 and 24–27. The larger $H_{1-2}O^{+\cdot}$ signals for $\mathbf{1}^{+\cdot}$ and $\mathbf{2}^{+\cdot}$ are consistent with their OH-carrying structures, from which water can be eliminated more readily than from keto structure $\mathbf{3}^{+\cdot}$ [48]. Comparison of the CAD and $^+N_fR^+$ data (Figures 4 and 7) further points out that most water is cleaved upon the decomposition $C_3H_6O^{+\cdot} \rightarrow C_3H_3^+$ (m/z 39) + H_2O + $^{\cdot}H$. Similarly, the dissociation $C_3H_6O^{+\cdot} \rightarrow {}^+CH_2OH$ (m/z 31) + $^{\cdot}C_2H_3$, which is much more pronounced for $\mathbf{1}^{+\cdot}$ and $\mathbf{2}^{+\cdot}$ than for $\mathbf{3}^{+\cdot}$ (viz. Figure 4), must be the major source of the enhanced relative intensities of $C_2H_{0-3}^+$ (m/z 24–27) in the $^+N_fR^+$ spectra of $\mathbf{1}^{+\cdot}$ and $\mathbf{2}^{+\cdot}$ (Figure 7).

The most abundant peak in all three $^+N_fR^+$ spectra appears at m/z 28. A fraction of this product origi-

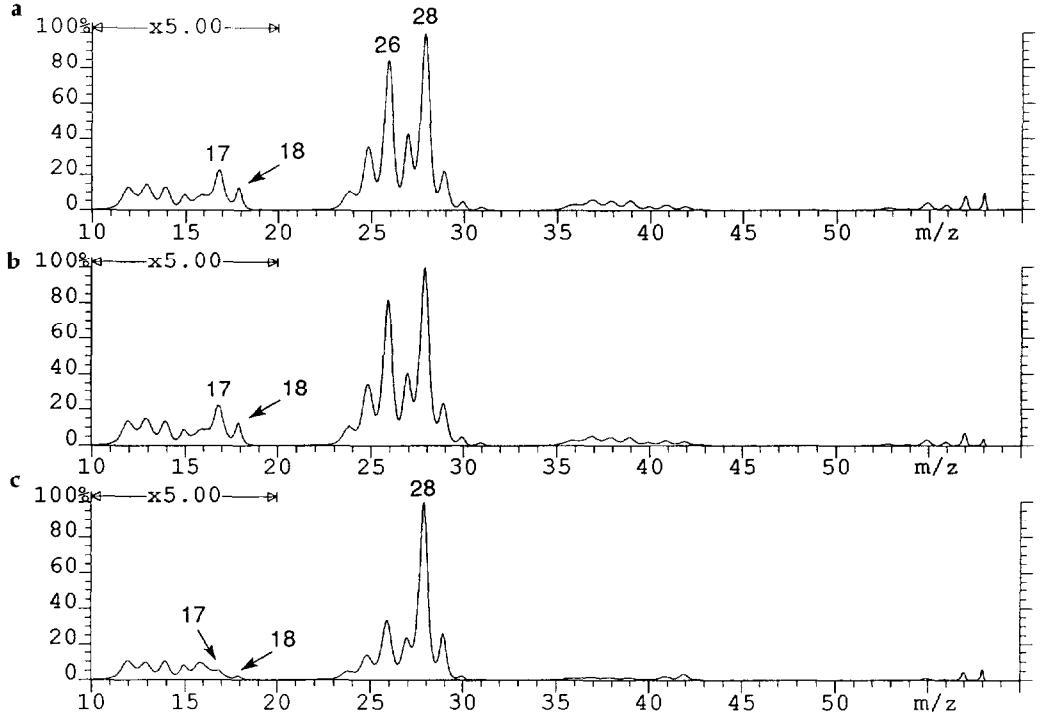

Figure 7. Neutral fragment–reionization ($^+N_fR^+$) spectra of (**a**) enol ion $CH_3CH{=}CHOH^{+\cdot}$ ($\mathbf{1}^{+\cdot}$), (**b**) distonic ion $^{\cdot}CH_2CH_2CH^+OH$ ($\mathbf{2}^{+\cdot}$), and (**c**) keto ion $CH_3CH_2CH{=}O^{+\cdot}$ ($\mathbf{3}^{+\cdot}$). These spectra contain the postionized neutral fragments eliminated upon CAD of $\mathbf{1}^{+\cdot}$–$\mathbf{3}^{+\cdot}$. The ionic fragments coproduced upon CAD of $\mathbf{1}^{+\cdot}$–$\mathbf{3}^{+\cdot}$ are shown in the spectra of Figure 4.

nates from the reaction $C_3H_6O^{+\cdot}$ ($\mathbf{1}^{+\cdot}$–$\mathbf{3}^{+\cdot}$) → $C_2H_6^{+\cdot}$ + CO (28 u), which is observed from all three tautomers (vide supra). Two other neutral CAD losses that can contribute (after postionization) to m/z 28 are the isobaric radicals $^{\cdot}CHO$ and $^{\cdot}C_2H_5$, cogenerated with $C_2H_5^+$ and ^+CHO (m/z 29 in the CAD spectra).

Neutralization–Reionization. The $^-NR^+$ spectrum of $\mathbf{3}^{+\cdot}$ also is markedly different from the spectra of $\mathbf{1}^{+\cdot}$ and $\mathbf{2}^{+\cdot}$ (Figure 8). Again, m/z 31 and 17 are much smaller for the keto ion $\mathbf{3}^{+\cdot}$ than for the OH-carrying ions $\mathbf{1}^{+\cdot}$ and $\mathbf{2}^{+\cdot}$. Other features of $\mathbf{3}^{+\cdot}$ that stand out are the high abundance of m/z 29 ($C_2H_5^+$ and ^+CHO) and the relatively low yield of $C_3H_3^+$ (m/z 39) and $C_2H_3O^+$ (m/z 43), as also seen on CAD. The unique CAD, $^+N_fR^+$, and $^-NR^+$ characteristics of $\mathbf{3}^{+\cdot}$ clearly indicate that propanal ions with insufficient energy for unimolecular decay (which are those sampled in CAD, $^+N_fR^+$, and $^-NR^+$ experiments [23–26]) do not readily isomerize to more stable $\mathbf{1}^{+\cdot}$ and/or $\mathbf{2}^{+\cdot}$. Based upon the [m/z 18]:[m/z 28] ratio in the $^+N_fR^+$ spectra (Figure 7) as well as the [m/z 31]:[m/z 29] ratio in the $^+NR^+$ spectra (Figure 8), less than 15% of nondecomposing propanal ions (lifetime > 10 μs) have interconverted to $\mathbf{1}^{+\cdot}$ and/or $\mathbf{2}^{+\cdot}$. In fact, the absence of molecular dications in the CAD spectrum of $\mathbf{3}^{+\cdot}$ demonstrates that no detectable amount of stable $CH_3CH_2CH{=}O^{+\cdot}$ (*which cannot dissociate*) rearranges to distonic or enolic structures. On the other hand, propanal ions that have been collisionally activated above their dissociation threshold *do interconvert* with $\mathbf{1}^{+\cdot}$ and/or $\mathbf{2}^{+\cdot}$ to some extent, as attested by the coformation of $CH_2{=}CHCH^+OH$ (m/z 57) and the formation of some $^+CH_2OH$ (31), $H_2O^{+\cdot}$ (18), and OH^+ (17) upon CAD (vide supra).

The behavior of $\mathbf{3}^{+\cdot}$ sharply contrasts to that of the homologous butanal ion, $CH_3CH_2CH_2CH{=}O^{+\cdot}$, which to a large extent rearranges spontaneously to the distonic ion $^{\cdot}CH_2CH_2CH_2CH^+OH$ [27, 28]. This difference most likely arises from the lower critical energy of the 1,5-H migration

$$H{-}CH_2CH_2\,CH_2CH{=}O^{+\cdot} \rightarrow {}^{\cdot}CH_2CH_2CH_2CH^+O{-}H$$

vis à vis that of the 1,4-migration

$$H{-}CH_2CH_2CH{=}O^{+\cdot}\ (\mathbf{3}^{+\cdot}) \rightarrow {}^{\cdot}CH_2CH_2CH^+O{-}H\ (\mathbf{2}^{+\cdot})\quad [17].$$

Distinguishing between tautomers $\mathbf{1}^{+\cdot}$ and $\mathbf{2}^{+\cdot}$ is a much more difficult task. As previously mentioned, their CAD (Figure 4a and b) and $^+N_fR^+$ (Figure 7a and b) spectra are practically identical. Their $^+NR^+$ spectra are similar too (Figure 8a and b), but include three discrete characteristics:

1. The absolute intensity of neutralized–reionized $C_3H_6O^{+\cdot}$ at m/z 58 ("recovery peak" or "survivor

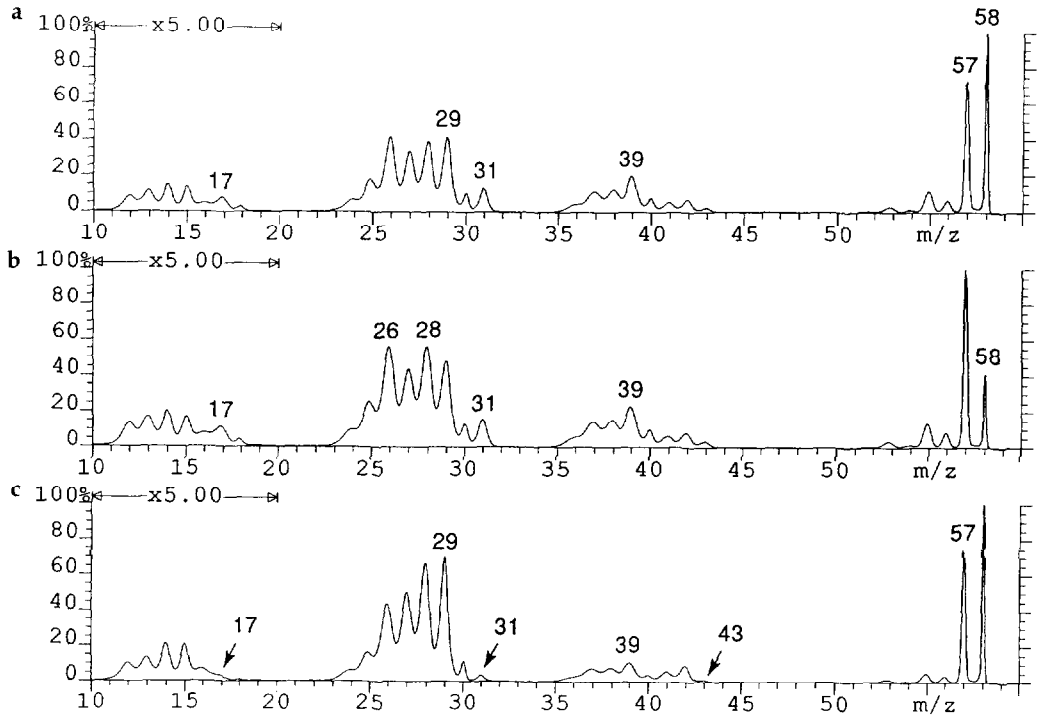

Figure 8. Neutralization–reionization ($^+NR^+$) spectra of (**a**) enol ion $CH_3CH{=}CHOH^{+\cdot}$ ($\mathbf{1}^{+\cdot}$), (**b**) distonic ion $^{\cdot}CH_2CH_2CH^+OH$ ($\mathbf{2}^{+\cdot}$), and (**c**) keto ion $CH_3CH_2CH{=}O^{+\cdot}$ ($\mathbf{3}^{+\cdot}$). The absolute abundances (i.e., $^+NR^+$ yields) of the recovery peaks (survivor ions) are 9×10^{-4} for (a) 9×10^{-5} for (b) and 7×10^{-4} for (c). The spectra were obtained with 70-eV EI and do not change outside experimental error if the electron energy is reduced to 15 eV.

ion'') is significantly higher for the enol ion than for the distonic ion.
2. The ratio $[C_3H_6O^{+\cdot}]:[C_3H_5O^+]$ is much greater for $\mathbf{1}^{+\cdot}$ (1.4) than for $\mathbf{2}^{+\cdot}$ (0.41; peak heights used in both cases).
3. The abundance pattern of m/z 26–29 from $^+NR^+$ of $\mathbf{2}^{+\cdot}$, namely, $[m/z\ 26] > [m/z\ 27] < [m/z\ 28] > [m/z\ 29]$, is slightly, yet reproducibly, different from the pattern observed from $\mathbf{1}^{+\cdot}$, namely, $[m/z\ 26] > [m/z\ 27] < [m/z\ 28] < [m/z\ 29]$.

Changing the internal energy of precursor ion $\mathbf{1}^{+\cdot}$ by forming it from different compounds, does not alter appreciably the described features. For example, $^+NR^+$ of $C_3H_6O^{+\cdot}$ from 2-methylbutanal, 2-methylpentanal (Figure 8a), 2-methylundecanal, *n*-pentanal, and *n*-hexanal (which have been shown to yield isomerically pure $\mathbf{1}^{+\cdot}$ [7, 11, 12, 17, 44]) gives rise to $[C_3H_6O^{+\cdot}]:[C_3H_5O^+]$ ratios of 2.0, 1.4, 1.5, 2.4, and 1.6, respectively. These ratios are markedly larger than the value obtained for $\mathbf{2}^{+\cdot}$ (0.41). Obviously, the differences between Figure 8a and b are not caused by internal energy effects but rather originate from the different structures of ions $\mathbf{1}^{+\cdot}$ and $\mathbf{2}^{+\cdot}$. The smaller survivor ion for $\mathbf{2}^{+\cdot}$ most probably results from the less favorable Franck–Condon factor of the redox sequence $\mathbf{2}^{+\cdot} \rightarrow \mathbf{2}$ (diradical) $\rightarrow \mathbf{2}^{+\cdot}$ vis à vis the sequence $\mathbf{1}^{+\cdot} \rightarrow \mathbf{1}$ (closed-shell enol) $\rightarrow \mathbf{1}^{+\cdot}$ [23–26].

Overall, our combined tandem mass spectrometry experiments provide sufficient information to determine the fate of the incipient distonic ion $\mathbf{2}^{+\cdot}$ that arises from HBL (eq 4). According to the CAD spectra (Figure 4), this ion either maintains its original structure or rearranges to $\mathbf{1}^{+\cdot}$; contamination by other, known $C_3H_6O^{+\cdot}$ isomer(s) can be excluded [7–14, 20, 21, 31, 43, 51]. The MI data (Figure 1) further point out that the $[HBL-CO_2]^{+\cdot}$ beam cannot be (entirely) $\mathbf{1}^{+\cdot}$. This is confirmed by the $^+NR^+$ spectrum of $[HBL-CO_2]^{+\cdot}$ (Figure 8b), which is characteristic of structure $\mathbf{2}^{+\cdot}$ (vide supra). In addition, the unique MI and $^+NR^+$ features assigned to ion $\mathbf{2}^{+\cdot}$ are reproduced when this ion is generated from other logical precursors (see next section). Based on all these facts, we conclude that distonic ion $\mathbf{2}^{+\cdot}$ is a distinct $C_3H_6O^{+\cdot}$ isomer, as proposed by theory [5, 6] and suggested by the previous studies of McAdoo and co-workers [8–10, 12]. Consequently, the similarity of the CAD, $^+N_fR^+$, and (to a lesser degree) $^+NR^+$ spectra of $\mathbf{1}^{+\cdot}$ and $\mathbf{2}^{+\cdot}$ must result from the dissociation of these two ions through common intermediates. It is interesting that the biggest spectral difference between $\mathbf{1}^{+\cdot}$ and $\mathbf{2}^{+\cdot}$ is observed in the relative and absolute abundances of the survivor ion (Figure 8a and b), whose generation involves gas-phase redox reactions but no dissociation.

Other Precursors for Distonic Ion $^{\cdot}CH_2CH_2CH\ ^+OH$ ($2^{+\cdot}$)

In the search for the best precursor for distonic ion $\mathbf{2}^{+\cdot}$, several linear and cyclic compounds were investigated (Tables 1 and 2). With the exception of HBL (eq 4), all other compounds considered were found to coproduce

Table 2. Partial CAD and $^+NR^+$ spectra of $C_3H_6O^{+\cdot}$ isomers

Precursor	CAD[a] $\frac{[m/z\ 43]}{[m/z\ 39]}$	$^+NR^+$[a] $\frac{[m/z\ 43]}{[m/z\ 39]}$	$\frac{[m/z\ 58]}{[m/z\ 57]}$	Base peak	Assigned structure
2-Methylpentanal	0.18	0.12	1.4	58	$\mathbf{1}^{+\cdot}$
α-Hydroxy-γ-butyrolactone (HBL)	0.21	0.15	0.41	57	$\mathbf{2}^{+\cdot}$
Propanal	0.16	0.10	1.4	58	$\mathbf{3}^{+\cdot}$
Methoxyacetone	2.2	1.7	13	58	$\mathbf{6}^{+\cdot}$
Methyl vinyl ether	59	29	33	58	$\mathbf{7}^{+\cdot}$
Cyclopentanol (CP)	0.52	0.26	1.2	58	$\mathbf{2}^{+\cdot}$ & $\mathbf{6}^{+\cdot}$[b]
3-Methoxypropanal (MEP)	1.2	0.71	1.2	58	$\mathbf{2}^{+\cdot}$ & $\mathbf{7}^{+\cdot}$[b]
4-Methylcyclohexanol (MCH)[c]	0.18	0.11	1.1	58	$\mathbf{1}^{+\cdot}$ & $\mathbf{2}^{+\cdot}$ & $\mathbf{6}^{+\cdot}$
3-Hydroxytetrahydrofuran (HTF)	0.24	0.15	0.57	57	$\mathbf{2}^{+\cdot}$ & $\mathbf{6}^{+\cdot}$
3-Methoxypropan-1-ol (MP)	0.24	0.14	0.61	57	$\mathbf{2}^{+\cdot}$ & $\mathbf{7}^{+\cdot}$
2-Methylbutanal[c]	0.21	0.11	2.0[d]	58	$\mathbf{1}^{+\cdot}$
2-Methylundecanal[c]	0.19	0.14	1.5[d]	58	$\mathbf{1}^{+\cdot}$
n-Pentanal[c]	0.20	0.13	2.4[d]	58	$\mathbf{1}^{+\cdot}$
n-Hexanal[c]	0.31	0.14	1.6[d]	58	$\mathbf{1}^{+\cdot}$
Cyclopropanol	0.26	0.20	0.50	57	$\mathbf{2}^{+\cdot}$ & $\mathbf{6}^{+\cdot}$
Allyl alcohol	0.22	0.13	0.25	57	$\mathbf{2}^{+\cdot}$

[a] From peak heights.
[b] Some $\mathbf{1}^{+\cdot}$ also could be present; see text.
[c] These precursors coproduce measurable amounts of the isobaric $C_4H_{10}^{+\cdot}$ cation (viz. Table 1). Based on its CAD and $^+NR^+$ spectra, $C_4H_{10}^{+\cdot}$ may affect $[m/z\ 43]$ and $[m/z\ 39]$, but does not contribute appreciably to the $^+NR^+$ peaks at m/z 58 and 57.
[d] The abundance pattern for m/z 26–29 is identical to that in Figure 8a, that is, $[m/z\ 26] > [m/z\ 27] < [m/z\ 28] < [m/z\ 29]$.

propanal enol ion ($\mathbf{1}^{+\cdot}$), acetone enol ion ($\mathbf{6}^{+\cdot}$), or methyl vinyl ether cation ($\mathbf{7}^{+\cdot}$). Ion $\mathbf{1}^{+\cdot}$ was discussed in detail in the preceding text. The tandem mass spectrometry characteristics of the putative contaminants $\mathbf{6}^{+\cdot}$ and $\mathbf{7}^{+\cdot}$ were established in previous studies [17, 20, 21, 52–54]. Here, we briefly present their most distinctive properties, which were used in the inquiry on the composition of the $C_3H_6O^{+\cdot}$ beams studied.

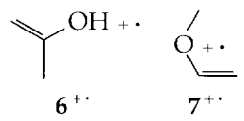

$\mathbf{6}^{+\cdot}$ $\mathbf{7}^{+\cdot}$

Metastable $\mathbf{6}^{+\cdot}$ and $\mathbf{7}^{+\cdot}$ lose $^{\cdot}CH_3$ to form the acetyl cation. The peak shapes and kinetic energy releases that result from this fragmentation are significantly different for the two isomers: $\mathbf{6}^{+\cdot}$ gives rise to a relatively broad gaussian signal with $T_{0.5} \approx 100$ meV, whereas $\mathbf{7}^{+\cdot}$ leads to an even wider, nongaussian signal with $T_{0.5} \approx 600$ meV (Figure 9a and b). Both the CAD (not shown) and $^{-}NR^{+}$ spectra (Figure 10) of $\mathbf{6}^{+\cdot}$ and $\mathbf{7}^{+\cdot}$ contain more abundant m/z 43 fragments than the respective spectra of isomers $\mathbf{1}^{+\cdot}$–$\mathbf{3}^{+\cdot}$. Finally, the $^{+}NR^{+}$ recovery peaks (m/z 58) of ions $\mathbf{6}^{+\cdot}$ and $\mathbf{7}^{+\cdot}$ are substantially larger than the peaks of distonic ion $\mathbf{2}^{+\cdot}$ (Figure 10 versus Figure 8b).

Cyclopentanol (CP). Ionized cyclopentanol can yield $\mathbf{2}^{+\cdot}$ by loss of ethylene (eq 2). The MI spectrum of the so-produced $C_3H_6O^{+\cdot}$ ion (Table 1) contains m/z 57 and 30 fragments, as did the spectrum of $\mathbf{2}^{+\cdot}$ from HBL (Figure 1b). However, also present is a sizable m/z 43 peak whose shape and width match those observed for m/z 43 from metastable acetone enol cation $\mathbf{6}^{+\cdot}$ (viz. Figure 9a). The additional fragment suggests that cyclopentanol coproduces $\mathbf{2}^{+\cdot}$ and $\mathbf{6}^{+\cdot}$. This is corroborated by the CAD and $^{+}NR^{+}$ spectra of $[CP-C_2H_4]^{+\cdot}$, both of which display more m/z 43 than the corresponding spectra of pure $\mathbf{2}^{+\cdot}$ (Table 2). The relatively large intensity of the survivor ion (m/z 58) in the $^{+}NR^{+}$ spectrum of $[CP-C_2H_4]^{+\cdot}$ (cf. Table 2) also agrees well with the presence of some $\mathbf{6}^{+\cdot}$ in the $[CP-C_2H_4]^{+\cdot}$ beam.

The appearance energy of $[CP-C_2H_4]^{+\cdot}$, measured by Holmes and Lossing [44], indicates that the $C_3H_6O^{+\cdot}$ isomer formed at threshold has a heat of formation of 661 kJ mol^{-1}. This value matches $\Delta H_f^{\circ}(\mathbf{6}^{+\cdot}) = 661$ kJ mol^{-1} [15], which corroborates that the $C_3H_6O^{+\cdot}$ beam from cyclopentanol contains $\mathbf{6}^{+\cdot}$. However, the MI, CAD, and $^{+}NR^{+}$ data of $[CP-C_2H_4]^{+\cdot}$ cannot exclude that CP ionization at 70 eV coproduces a small amount of $\mathbf{1}^{+\cdot}$ (together with $\mathbf{2}^{+\cdot}$ and $\mathbf{6}^{+\cdot}$). The most prominent property of isomer $\mathbf{1}^{+\cdot}$ is the high abundance of its survivor ion upon $^{+}NR^{+}$ (vide supra). Unfortunately, this feature is obscured by the presence of $\mathbf{6}^{+\cdot}$, which also gives rise to an abundant recovery peak (viz. Figure 10a).

3-Methoxypropanal (MEP). The first experimental data reported on $\mathbf{2}^{+\cdot}$ were obtained from cations generated from 3-methoxypropanal [12]. This molecule can lead to the distonic ion $^{\cdot}CH_2CH_2CH^{+}OH$ via a δ-H rearrangement, followed by $CH_2{=}O$ loss (eq 3a). The corresponding MI spectrum duplicates all features of Figure 1b and, additionally, shows a broad nongaussian m/z 43 fragment with a shape and $T_{0.5}$ that are very similar to those obtained from metastable methyl vinyl ether ion $\mathbf{7}^{+\cdot}$ (Figure 9b). The presence of $\mathbf{7}^{+\cdot}$ in the $[MEP-CH_2{=}O]^{+\cdot}$ beam is further verified by the CAD and $^{+}NR^{+}$ spectra of the latter cation (Figure 11). These include a larger m/z 43 signal than the respective spectra of $\mathbf{2}^{+\cdot}$ (Figures 4b and 8b). The admixture of $\mathbf{7}^{+\cdot}$ also raises the abundance of the survivor ion above the amount that can be supplied by pure $\mathbf{2}^{+\cdot}$ (cf. Figure 11b versus Figure 8b). Ion $\mathbf{7}^{+\cdot}$ could be formed from $MEP^{+\cdot}$ as rationalized in eq 3b, that is, via a 1,2-CH_2O elimination.

3-Methoxypropanal can be envisaged as a 1,2-disubstituted ethane, $CH_3O-CH_2CH_2-CHO$. The related 1,2-disubstituted ethane

$$CH_3O-CH_2CH_2-OH$$

also yields some $\mathbf{7}^{+\cdot}$ (nominal 1,2-H_2O loss); the major product is the distonic ion $^{+}CH_2OCH_2CH_2^{\cdot}$ (nominal

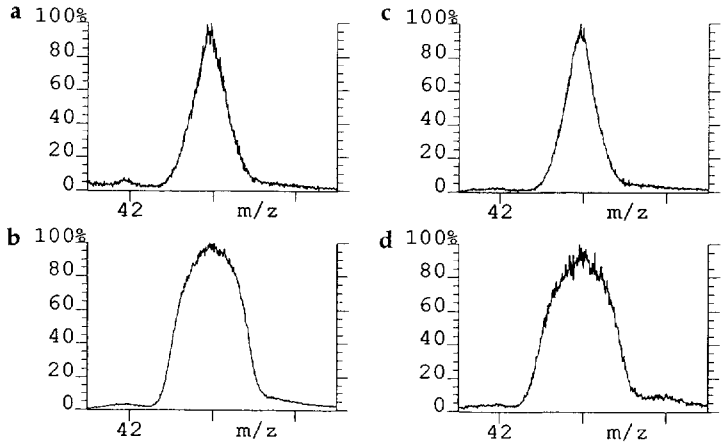

Figure 9. The m/z 43 peak in the MI spectra of (**a**) acetone enol ion $CH_2{=}C(CH_3)OH^{+\cdot}$ ($\mathbf{6}^{+\cdot}$), (**b**) methyl vinyl ether ion $CH_3OCH{=}CH_2^{+\cdot}$ ($\mathbf{7}^{+\cdot}$), and the $C_3H_6O^{+\cdot}$ ions from (**c**) 3-hydroxytetrahydrofuran, $[HTF-CH_2{=}O]^{+\cdot}$, and (**d**) 3-methoxypropan-1-ol, $[MP-CH_3OH]^{+\cdot}$ (eq 6).

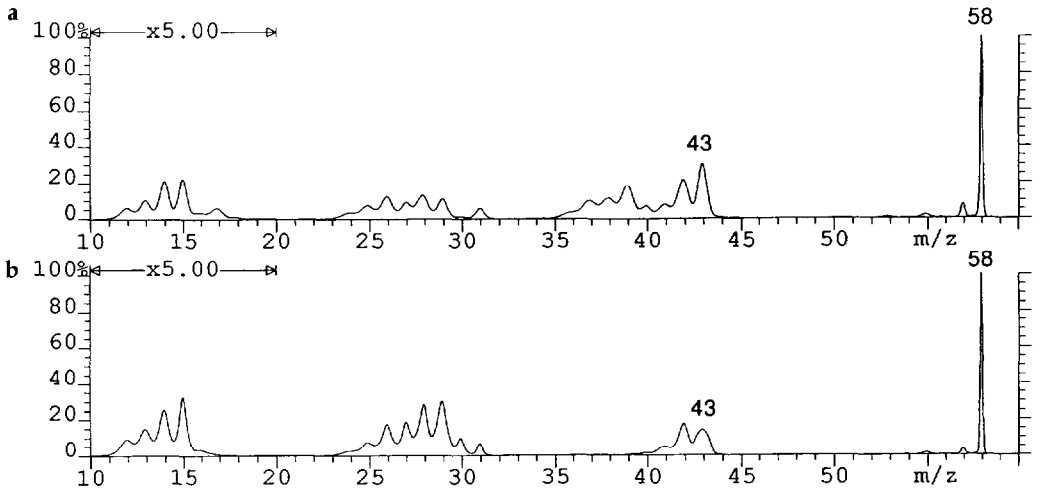

Figure 10. $^{+}NR^{+}$ spectra of (a) enol ion $CH_2{=}C(CH_3)OH^{+\cdot}$ ($\mathbf{6}^{+\cdot}$; from methoxyacetone) and (b) ion $CH_3OCH{=}CH_2^{+\cdot}$ ($\mathbf{7}^{+\cdot}$; from methyl vinyl ether).

1,4-H_2O loss) [21]. Finally, it should be pointed out that, for the reason given for the cyclopentanol precursor, the MI, CAD, and $^{+}NR^{+}$ spectra of $C_3H_6O^{+\cdot}$ from MEP cannot preclude that ions formed at 70 eV contain a small amount of enol isomer $\mathbf{1}^{+\cdot}$ too. The appearance energy measurements of Traeger et al. [12] connote, however, that $\mathbf{1}^{+\cdot}$ is not formed at threshold.

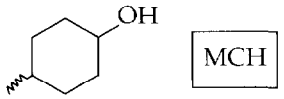

4-Methylcyclohexanol (MCH). The molecular ion of the cis and trans isomers of this compound decomposes by C_4H_8 loss to yield a $C_3H_6O^{+\cdot}$ ion, whose CAD spectrum is very similar to spectra of ions $\mathbf{1}^{+\cdot}$ and $\mathbf{2}^{+\cdot}$ (remember that $\mathbf{1}^{+\cdot}$ and $\mathbf{2}^{+\cdot}$ are indistinguishable by CAD; vide supra). The appearance of CAD products at m/z 48–51 ($C_4H_{0-3}^{+}$) documents that 4-methylcyclohexanol cogenerates an appreciable amount of the isobaric $C_4H_{10}^{+\cdot}$ cation. This fact is confirmed by the MI spectrum (Table 1) that contains a sizable m/z 42 signal (CH_4 loss), as does the reference MI spectrum of pure $C_4H_{10}^{+\cdot}$. The MI fragments at m/z 57 and 30 point out that the $C_3H_6O^{+\cdot}$ component has partly the distonic structure $\mathbf{2}^{+\cdot}$, which can arise from $MCH^{+\cdot}$ by ring opening and subsequent cleavage of C_4H_8 [13]. The relative abundance of the recovery peak and the m/z 26–29 intensity pattern in the $^{+}NR^{+}$ spectrum (Figure 12a) further show that $\mathbf{1}^{+\cdot}$ may be formed from MCH, too. Moreover, the trace of gaussian m/z 43

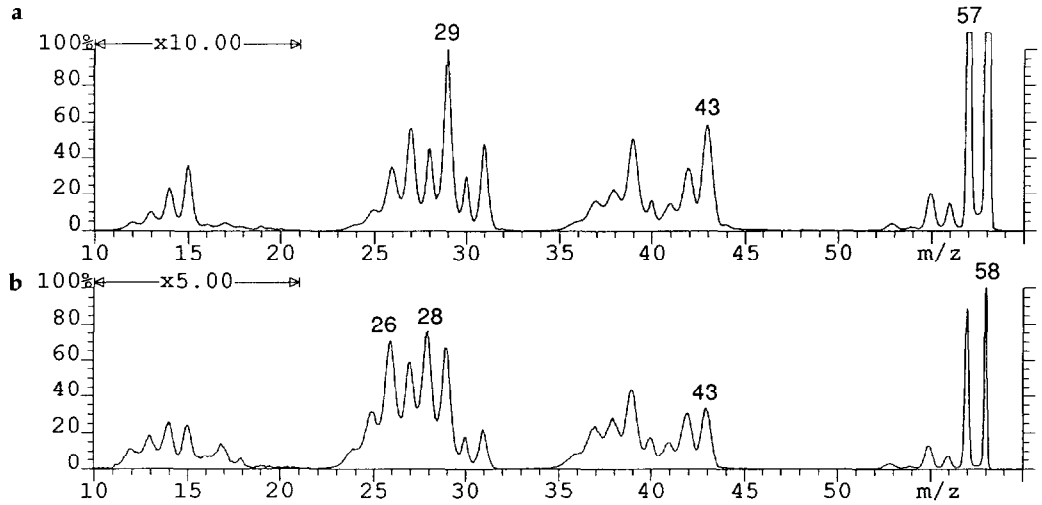

Figure 11. (a) CAD and (b) $^{+}NR^{+}$ spectra of the $C_3H_6O^{+\cdot}$ ion from 3-methoxypropanal, $[MEP{-}CH_2{=}O]^{+\cdot}$. The abundance of m/z 57 in the CAD spectrum is 526% relative to [m/z 29].

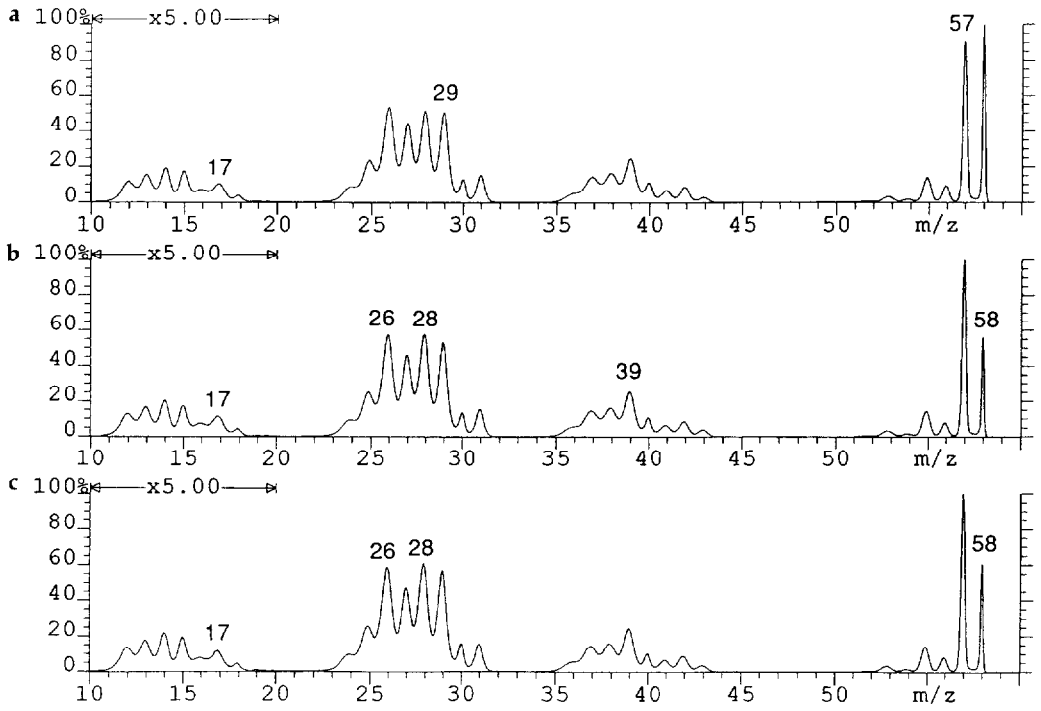

Figure 12. $^+NR^-$ spectra of $C_3H_6O^{+\cdot}$ from (**a**) *trans*-4-methylcyclohexanol, $[MCH-C_4H_8]^{+\cdot}$, (**b**) 3-hydroxytetrahydrofuran, $[HTF-CH_2{=}O]^{+\cdot}$, and (**c**) 3-methoxypropan-1-ol, $[MP-CH_3OH]^{+\cdot}$. $[MCH-C_4H_8]^{+\cdot}$ from *cis*-4-methylcyclohexanol gives rise to a spectrum that is identical within experimental error to that in part a.

observed in the MI spectrum (Table 1) suggests that a third isomer, namely, $\mathbf{6}^{+\cdot}$, also is contained in the $[MCH-C_4H_8]^{+\cdot}$ beam.

In contrast to earlier reports by Gu and Turecek [13], we find that the stereochemistry of MCH (cis or trans) has no visible effect on the $^+NR^+$ spectrum of its $C_3H_6O^{+\cdot}$ fragment. Also, our $^+NR^+$ spectrum of $[MCH-C_4H_8]^{+\cdot}$ differs from that reported [13], which rather resembles an $^+N_fR^+$ spectrum (viz. Figure 7a and b). This discrepancy may arise from the use of different mass analyzers in the product ion analysis (electric sector by us versus quadrupole mass filter by Gu and Turecek) or by different CAD versus neutralization efficiencies with the two instruments.

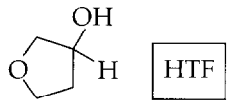

3-Hydroxytetrahydrofuran (HTF). The $^+NR^+$ spectrum of the $C_3H_6O^{+\cdot}$ cation from HTF ($CH_2{=}O$ loss) is strikingly similar to that of $\mathbf{2}^{+\cdot}$ from HBL (cf. Figure 12b versus Figure 8b). The only detectable difference between these two spectra is the slightly (but reproducibly) more abundant recovery peak for $[HTF-CH_2O]^{+\cdot}$ (Figure 12b) as compared to $[HBL-CO_2]^{+\cdot}$ (Figure 8b). The MI spectrum of $[HTF-CH_2O]^{+\cdot}$ shows m/z 57 and 30 fragments (Table 1), which (together) are diagnostic for the distonic isomer $\mathbf{2}^{+\cdot}$, but also includes a small peak at m/z 43 (Figure 9c) with a shape similar to that of Figure 9a, which is indicative of enolic isomer $\mathbf{6}^{+\cdot}$. Hence, the combined MI and $^+NR^+$ data suggest that HTF gives rise to a $C_3H_6O^{+\cdot}$ mixture composed of predominantly $\mathbf{2}^{+\cdot}$ plus a very small amount of $\mathbf{6}^{+\cdot}$.

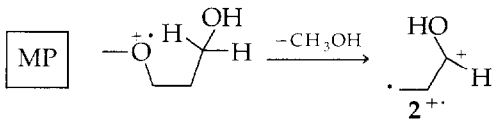

(6)

3-Methoxypropan-1-ol (MP). 3-Methoxypropan-1-ol, the saturated analog of MEP (viz. eq 3a), nominally yields $\mathbf{2}^{+\cdot}$ via a γ-H rearrangement followed by methanol loss (viz. eq 6). The $^+NR^+$ spectrum of $[MP-CH_3OH]^{+\cdot}$ (Figure 12c) is very similar to that of $C_3H_6O^{+\cdot}$ from 3-hydroxytetrahydrofuran (Figure 12b). It is evident CH_3OH loss from $MP^{+\cdot}$ *mainly* leads to $\mathbf{2}^{+\cdot}$, as did CH_2O loss from $HTF^{+\cdot}$ (vide supra). However, comparison of the MI spectrum of $[MP-CH_3OH]^{+\cdot}$ to that of methyl vinyl ether ion (Figure 9d versus 9b) reveals that, *in this case*, some $\mathbf{7}^{+\cdot}$ is coproduced; its presence can account for the slightly larger recovery peak in the $^+NR^+$ spectrum of $[MP-CH_3OH]^{+\cdot}$ (Figure 12c) vis à vis the spectrum of pure $\mathbf{2}^{+\cdot}$ (Figure 8b).

In addition to the preceding compounds, four potential precursors of enol ion $\mathbf{1}^{+\cdot}$ were examined,

namely, 2-methylbutanal, 2-methylundecanal, *n*-pentanal, and *n*-hexanal. These four samples yield $\mathbf{1}^{+\cdot}$ according to earlier mass spectrometry [55], tandem mass spectrometry [7], or appearance energy studies [44]. This is confirmed by our MI, CAD, and $^{+}NR^{+}$ data (Tables 1 and 2). We also find that the foregoing four molecules cogenerate detectable quantities of the isobaric $C_4H_{10}^{+\cdot}$ ion and, therefore, are less suitable precursors of $\mathbf{1}^{+\cdot}$, compared to 2-methylpentanal.

The preceding discussion illustrates that combination of the information stored in various types of tandem mass spectra offers a particularly powerful tool for analysis of isomeric (and isobaric) ion mixtures. It also emphasizes the problems encountered in the search for an adequate source for distonic ion $\mathbf{2}^{+\cdot}$. All cyclic precursors considered (by us and others) contain the connectivity of $\mathbf{2}^{+\cdot}$ and would lead to this isomer by a least-motion extrusion [56] of a stable neutral molecule. Also linear MEP and the other linear precursors investigated (vide supra) would produce $\mathbf{2}^{+\cdot}$ by simple γ- or δ-H rearrangements followed by scission of a stable molecule. Yet, almost all precursors (except HBL) cogenerate readily detectable amounts of isomers $\mathbf{1}^{+\cdot}$, $\mathbf{6}^{+\cdot}$, or $\mathbf{7}^{+\cdot}$ (whose formation involves more complicated molecular reorganizations).

HBL, the best precursor found for $\mathbf{2}^{+\cdot}$ (eq 4), does not yield any $\mathbf{6}^{+\cdot}$ or $\mathbf{7}^{+\cdot}$. Whether the $C_3H_6O^{+\cdot}$ ion from this compound is contaminated with some $\mathbf{1}^{+\cdot}$ is more difficult to decipher with the experimental methods available to us. The main reason for this difficulty is that $\mathbf{1}^{+\cdot}$ does not form a unique fragment (in its MI, CAD, or $^{+}NR^{+}$ spectra) that is not produced also from $\mathbf{2}^{+\cdot}$. This aspect will be discussed in more detail in the section about the diradical $^{\cdot}CH_2CH_2CH^{\cdot}OH$ (neutralized $\mathbf{2}^{+\cdot}$).

Structure of Ionized Cyclopropanol ($4^{+\cdot}$) and Allyl Alcohol ($5^{+\cdot}$)

The major decomposition pathway of metastable $\mathbf{4}^{+\cdot}$ and $\mathbf{5}^{+\cdot}$ leads to $C_3H_5O^{+}$ (m/z 57) by loss of $H^{\cdot}$ (Table 1). A second, minor dissociation channel proceeds by expulsion of CO to give rise to $C_2H_6^{+\cdot}$ at m/z 30 (composition established by MS/MS/MS). Such MI characteristics are indicative of distonic ion $\mathbf{2}^{+\cdot}$ (viz. Figure 1b), suggesting that dissociating $\mathbf{4}^{+\cdot}$ and $\mathbf{5}^{+\cdot}$ readily equilibrate to $\mathbf{2}^{+\cdot}$, which can be reached from $\mathbf{4}^{+\cdot}$ and $\mathbf{5}^{+\cdot}$ by ring opening (eq 7) or 1,2-hydride shift (eq 8), respectively. The MI spectrum of $\mathbf{4}^{+\cdot}$ also includes a peak at m/z 43 that has the same shape and $T_{0.5}$ as the m/z 43 peak from enolic $\mathbf{6}^{+\cdot}$. Hence, some metastable $\mathbf{4}^{+\cdot}$ has isomerized to $\mathbf{6}^{+\cdot}$, possibly via the route shown in eq 9; alternatively, $\mathbf{6}^{+\cdot}$ could already have been preformed in the ion source during the ionization process.

Metastable $\mathbf{4}^{+\cdot}$ and $\mathbf{5}^{+\cdot}$ yield gaussian m/z 30 signals. In contrast, the m/z 30 signal from metastable $\mathbf{2}^{+\cdot}$ (Figure 1b) has a flatter top and more vertical sides. We reported in the preceding text that the peak shape of m/z 30 from $\mathbf{2}^{+\cdot}$ changes to gaussian on collisional activation (Figure 4b), presumably because of a different fragmentation mechanism at elevated internal energies. Based on the known heats of formation of $\mathbf{4}^{+\cdot}$ (786 kJ mol^{-1}) [15] and $\mathbf{5}^{+\cdot}$ (808 kJ mol^{-1}) [15] and the predicted ΔH_f° value of $\mathbf{2}^{+\cdot}$ ($\leq$ 760 kJ mol^{-1}) ([6] and Bouchoux, G., private communication) the isomerizations $\mathbf{4}^{+\cdot} \rightarrow \mathbf{2}^{+\cdot}$ and $\mathbf{5}^{+\cdot} \rightarrow \mathbf{2}^{+\cdot}$ are exothermic by at least 26 and 48 kJ mol^{-1}, respectively, thereby producing internally excited $\mathbf{2}^{+\cdot}$. Apparently, this extra internal energy is sufficient to promote dissociation via the mechanism that leads to the gaussian m/z 30 signal.

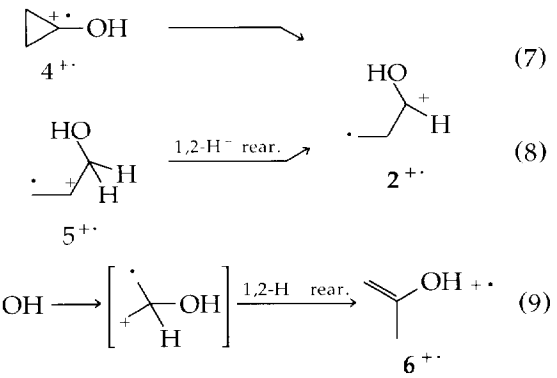

The CAD spectra of $\mathbf{4}^{+\cdot}$ and $\mathbf{5}^{+\cdot}$ are identical within experimental error [31] and indistinguishable from the corresponding spectra of ions $\mathbf{1}^{+\cdot}$ and $\mathbf{2}^{+\cdot}$ (Figure 4a and b). On the other hand, the $^{+}NR^{+}$ spectra of $\mathbf{4}^{+}$ and $\mathbf{5}^{+\cdot}$ (Figure 13) are very similar to the $^{+}NR^{+}$

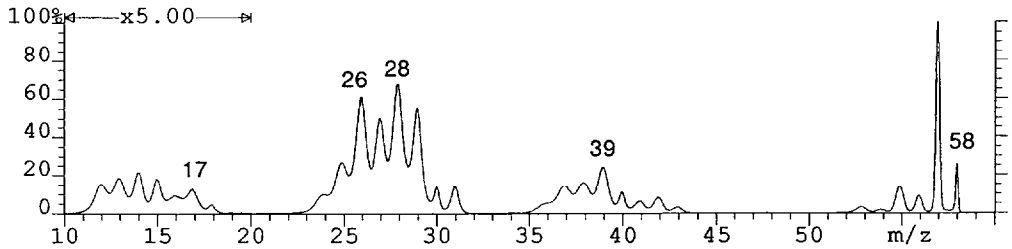

Figure 13. $^{-}NR^{+}$ spectrum of allyl alcohol ion ($\mathbf{5}^{+\cdot}$). The cyclopropanol ion ($\mathbf{4}^{+\cdot}$) gives rise to a spectrum with very similar fragment ion abundances but a more abundant survivor ion (viz. Table 2). The spectra do not change outside experimental error if the energy of the ionizing electrons is reduced from 70 to 15 eV.

spectrum of distonic ion $\mathbf{2}^{+\cdot}$ (Figure 8b) and differ from the $^+NR^+$ spectrum of enol ion $\mathbf{1}^{+\cdot}$ in both the magnitude of the [m/z 58]:[m/z 57] ratio (Table 2) as well as the intensity pattern of the fragments between m/z 26 and 29. $^+NR^+$ probes ions that lack enough energy for spontaneous dissociation (stable ions). Hence, our $^+NR^+$ observations point out that stable $\mathbf{4}^{+\cdot}$ and $\mathbf{5}^{+\cdot}$ isomerize readily to $\mathbf{2}^{+\cdot}$ but not to $\mathbf{1}^{+\cdot}$. This result is in agreement with very recent ab initio calculations by Bouchoux (private communication) that find $\mathbf{4}^{+\cdot}$ to be a transition state in the rearrangement $^{\cdot}C^{\beta}H_2C^{\alpha}H_2CH^-OH$ $(\mathbf{2}^{+\cdot}) \rightarrow HO^+CHC^{\beta}H_2C^{\alpha}H_2^{\cdot}$ $(\mathbf{2'}^{+\cdot})$ and $\mathbf{5}^{+\cdot}$ to reside in a shallow well with a barrier of only 9 kJ mol^{-1} for the 1, 2-H$^-$ shift $\mathbf{5}^{+\cdot} \rightarrow \mathbf{2}^{+\cdot}$ (eq 8). For comparison, the predicted critical energies for $\mathbf{2}^{+\cdot} \rightarrow \mathbf{1}^{+\cdot}$ and $\mathbf{2}^{+\cdot} \rightarrow \mathbf{3}^{+\cdot}$ are markedly higher (Figure 3).

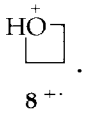

$\mathbf{8}^{+\cdot}$

As previously mentioned, the exothermic reactions 7 and 8 generate $\mathbf{2}^{+\cdot}$ at higher average internal energies. If this excitation is carried over (at least partly) to the survivor ion that arises upon $^+NR^+$, more extensive fragmentation could result, which would reduce the relative abundance of the survivor ion. Still, the [m/z 58]:[m/z 57] ratio observed for $\mathbf{4}^{+\cdot}$ is slightly (but reproducibly) higher than the ratio for authentic $\mathbf{2}^{+\cdot}$ (from HBL; viz. Table 2). This difference is ascribed to the presence of a small amount of $\mathbf{6}^{+\cdot}$ in $\mathbf{4}^{+\cdot}$ (vide supra). On the other hand, for $\mathbf{5}^{+\cdot}$, the [m/z 58]:[m/z 57] ratio is indeed smaller than that for genuine $\mathbf{2}^{+\cdot}$ (Table 2), as expected. We cannot exclude, however, that $\mathbf{5}^{+\cdot}$ has in part rearranged to another, yet unidentified, isomer that yields a very small survivor ion. A plausible candidate is the cyclic ion $\mathbf{8}^{+\cdot}$, which has been invoked as an intermediate in the fragmentation of ionized allyl alcohol [30].

Diradical $^{\cdot}CH_2CH_2CH^{\cdot}OH$

The appearance of a sizable recovery peak in the $^+NR^+$ spectrum of distonic ion $\mathbf{2}^{+\cdot}$ (Figure 8b) points out that the neutralized form of $\mathbf{2}^{+\cdot}$, that is the 1,3-diradical 2, is a bound species that resides in a potential energy minimum. Many other 1,3- and 1,4-diradicals have been found to be stable [21, 27, 43, 57, 58]. Nevertheless, we must note that the survivor ion in the $^+NR^+$ spectrum of $\mathbf{2}^{+\cdot}$ may partly originate from a small (but not detectable) amount of $\mathbf{1}^{+\cdot}$ in the $[HBL-CO_2]^{+\cdot}$ beam. The absolute abundance of m/z 58 in the $^+NR^+$ spectrum of $\mathbf{2}^{+\cdot}$ is 10% of the value measured for $\mathbf{1}^{+\cdot}$ (see legend of Figure 8). Consequently, $[HBL-CO_2]^{+\cdot}$ could contain up to 10% $\mathbf{1}^{+\cdot}$ (in addition to $\geq$ 90% $\mathbf{2}^{+\cdot}$).

The relative fragment ion abundances in the $^+NR^+$ spectra of $\mathbf{1}^{+\cdot}$ and $\mathbf{2}^{+\cdot}$ are fairly similar, as in the corresponding CAD spectra. This in turn suggests that the majority of the fragments observed in the $^+NR^+$ spectra result from ionic fragmentations (i.e., after reionization) [24–26, 57, 59]. It is evident that diradical **2** (ΔH_f° = 127 kJ mol^{-1} by additivity [60]) does not dissociate measurably in the $\sim$ 1 μs available between its synthesis (neutralization step) and detection (reionization step), otherwise, its $^+NR^+$ spectrum would differ significantly from that of the more stable enol **1** (ΔH_f° = $-$172 kJ mol^{-1} [15]). For comparison, the isomeric diradical $^{\cdot}CH_2CH_2OCH_2^{\cdot}$, which also is bound [43], was shown to decompose extensively to $CH_2{=}CH_2$ plus $O{=}CH_2$ [43]. The different reactivity of intermediate **2** may be caused by the need of energy demanding and hence slow H-rearrangement(s) for it to form any stable, closed-shell fragments.

The neutralization reaction can produce diradical 2 in either its singlet or triplet state. Singlet 2 could ring-close to cyclopropanol (ΔH_f° = $-$92 kJ mol^{-1} [15]), which is thermodynamically more stable than 2 [34, 35]. It is impossible to verify whether this happened within the time window of the experiment ($\sim$ 1 μs), because the $^+NR^+$ products from 2 and 4 are indistinguishable (vide supra).

Conclusions

In parallel with other $C_3H_6O^{+\cdot}$ radical cations with the CCCO frame [17], the distonic ion $^{\cdot}CH_2CH_2CH^+OH$ $(\mathbf{2}^{+\cdot})$ mainly decomposes to $H^{\cdot} + CH_3CH_2C{\equiv}O^+$ (m/z 57) both at threshold and when collisionally activated. At higher internal energies a small fraction of $CH_2{=}CHCH^+OH$ (m/z 57) is cogenerated. Analogous behavior is observed for enol ion $CH_3CH{=}CHOH^{+\cdot}$ $(\mathbf{1}^{+\cdot})$ [11]. The very similar CAD spectra of $\mathbf{1}^{+\cdot}$ and $\mathbf{2}^{+\cdot}$ further attest that, once excited, these two isomers dissociate through essentially the same pathways. This situation in turn compromises their differentiation by CAD.

Metastable $\mathbf{2}^{+\cdot}$ from several precursors undergoes a unique fragmentation (to $C_2H_6^{+\cdot} + CO$) that is not observed for isomer $\mathbf{1}^{+\cdot}$. In addition, the $^+NR^+$ spectra of $\mathbf{1}^{+\cdot}$ and $\mathbf{2}^{+\cdot}$ show a markedly distinct $[C_3H_6O^{+\cdot}]$:$[C_3H_5O^+]$ ratio. The MI and $^+NR^+$ features of $\mathbf{1}^{+\cdot}$ and $\mathbf{2}^{+\cdot}$ allow one to distinguish between these isomers, as was demonstrated for $C_3H_6O^{+\cdot}$ ions from a large number of linear and cyclic precursors. This study also has shown that the combined MI and $^+NR^+$ data of a given $C_3H_6O^{+\cdot}$ can serve as a fingerprint to deduce the origin of this $C_3H_6O^{+\cdot}$ cation (viz. Tables 1 and 2).

Several samples were found to produce isomerically pure $\mathbf{1}^{+\cdot}$, either via the McLafferty rearrangement (the 2-methylalkanals) or via more complicated reactions (pentanal and hexanal). In sharp contrast, many logical precursors for $\mathbf{2}^{+\cdot}$ generate admixtures of other isomers, specifically $\mathbf{1}^{+\cdot}$, $\mathbf{6}^{+\cdot}$ (enol ion of acetone), or $\mathbf{7}^{+\cdot}$

(ionized methyl vinyl ether). Generally, $\mathbf{6}^{+\cdot}$ and $\mathbf{7}^{+\cdot}$ are formed from molecules that contain the $CH_2CH(OH)CH_2$ substructure or a CH_3O group, respectively.

The CAD, $^{+}N_fR^{+}$, and $^{+}NR^{+}$ spectra of the propanal cation ($\mathbf{3}^{+\cdot}$) provide strong evidence that this ionized carbonyl maintains its original structure even several microseconds after its formation. Hence, the exothermic isomerizations $\mathbf{3}^{+\cdot} \rightarrow \mathbf{2}^{+\cdot}$ and $\mathbf{3}^{+\cdot} \rightarrow \mathbf{1}^{+\cdot}$ are associated with appreciable critical energies. Similarly, our tandem mass spectrometry data indicate that the exothermic reaction $\mathbf{2}^{+\cdot} \rightarrow \mathbf{1}^{+\cdot}$ also must surmount a sizable barrier. On the other hand, ionized cyclopropanol ($\mathbf{4}^{+\cdot}$) and allyl alcohol ($\mathbf{5}^{+\cdot}$) are found to spontaneously rearrange to $\mathbf{2}^{+\cdot}$, which, as the more stable isomer, should be the common structure; further isomerization to enol $\mathbf{1}^{+\cdot}$ does not take place.

Acknowledgments

We thank Fred A. Wiedmann and Dr. Michael J. Taschner for the synthesis of cyclopropanol and Dr. John C. Traeger for useful comments. We are indebted to Dr. David J. McAdoo and Dr. Charles E. Hudson for a sample of 3-methoxypropanal as well as helpful suggestions, Dr. Guy Bouchoux for providing us his newest theoretical data on the $C_3H_6O^{+\cdot}$ system, and Dr. Leo Radom for the G2 value of the propanoyl cation. This work was supported by the Petroleum Research Fund, which is Administered by the American Chemical Society, and the University of Akron.

References

1. McLafferty, F. W.; Stauffer, D. B. *Wiley/NBS Registry of Mass Spectral Data*; Wiley: New York, 1989.
2. Bouma, W. J.; MacLeod, J. K.; Radom, L. *J. Am. Chem. Soc.* **1980**, *102*, 2246–2252.
3. Hoppilliard, Y.; Bouchoux, G.; Jaudon, P. *Nouv. J. Chim.* **1982**, *6*, 43–52.
4. Bouchoux, G.; Hoppilliard, Y. *Int. J. Mass Spectrom. Ion Processes* **1983/1984**, *55*, 47–53.
5. Bouchoux, G.; Tortajada, J. *Rapid Commun. Mass Spectrom.* **1987**, *1*, 86–87.
6. Hudson, C. E.; McAdoo, D. J. *Tetrahedron* **1990**, *46*, 331–334.
7. Van de Sande, C. C.; McLafferty, F. W. *J. Am. Chem. Soc.* **1975**, *97*, 4617–4620.
8. McAdoo, D. J.; Witiak, D. N. *J. Chem. Soc., Perkin Trans. 2* **1981**, 770–773.
9. Hudson, C. E.; McAdoo, D. J. *Org. Mass Spectrom.* **1982**, *17*, 366–368.
10. Hudson, C. E.; McAdoo, D. J. *Org. Mass Spectrom.* **1984**, *19*, 1–6.
11. Turecek, F.; Hanus, V.; Gäumann, T. *Int. J. Mass Spectrom. Ion Processes* **1986**, *69*, 217–231.
12. McAdoo, D. J.; Hudson, C. E.; Traeger, J. C. *Org. Mass Spectrom.* **1988**, *23*, 760–764.
13. Gu, M.; Turecek, F. *Org. Mass Spectrom.* **1994**, *29*, 85–89.
14. McAdoo, D. J.; Hudson, C. E. *J. Mass Spectrom.* **1995**, *30*, 492–496.
15. (a) Lias, S. G.; Liebman, J. F.; Levin, R. D.; Kafafi, S. A. *NIST Standard Reference Database 25*, version 2.02, **1994**; (b) Lias, S. G.; Bartmess, J. E.; Liebman, J. F.; Holmes, J. L.; Levin, R. D.; Mallard, W. G. *J. Phys. Chem. Ref. Data* **1988**, Suppl. 1.
16. Wesdemiotis, C.; McLafferty, F. W. *Tetrahedron Lett.* **1981**, *22*, 3479–3480.
17. Bouchoux, G. *Mass Spectrom. Rev.* **1988**, *7*, 1–39.
18. Hammerum, S. *Mass Spectrom. Rev.* **1988**, *7*, 123–202.
19. Stirk, K. M.; Kiminkinen, M.; Kenttämaa, H. I. *Chem. Rev.* **1992**, *92*, 1649–1665.
20. Turecek, F.; McLafferty, F. W. *J. Am. Chem. Soc.* **1984**, *106*, 2528–2531.
21. Polce, M. J.; Wesdemiotis, C. *J. Am. Soc. Mass Spectrom.* **1995**, *6*, 1030–1036.
22. (a) Polce, M. J.; Wiedmann, F. A.; Wesdemiotis, C. *Proceedings of the 41st ASMS Conference*, San Francisco, CA, May 31–June 4, 1993, pp 283a–283b. (b) Polce, M. J.; Wesdemiotis, C. *Proceedings of the 42nd ASMS Conference*, Chicago, IL, May 29–June 3, 1994, p 206.
23. Busch, K. L.; Glish, G. L.; McLuckey, S. A. *Mass Spectrometry/Mass Spectrometry*; VCH Publishers, Inc.: New York, 1988.
24. Wesdemiotis, C.; McLafferty, F. W. *Chem. Rev.* **1987**, *87*, 485–500.
25. Terlouw, J. K.; Schwarz, H. *Angew. Chem. Int. Ed. Engl.* **1987**, *26*, 805–815.
26. Holmes, J. L. *Mass Spectrom. Rev.* **1989**, *8*, 513–539.
27. Polce, M. J.; Cordero, M. M.; Wesdemiotis, C.; Bott, P. A. *Int. J. Mass Spectrom. Ion Processes* **1992**, *113*, 35–58.
28. Bouchoux, G.; Alcaraz, C.; Dutuit, O.; Nguyen, M. T. *Int. J. Mass Spectrom. Ion Processes* **1994**, *137*, 93–106.
29. Zeller, L.; Farrell, J., Jr.; Vainiotalo, P.; Kenttämaa, H. I. *J. Am. Chem. Soc.* **1992**, *114*, 1205–1214.
30. Kurland, J. J.; Lutz, R. P. *J. Chem. Soc. Chem. Commun.* **1968**, 1097–1098.
31. Holmes, J. L.; Burgers, P. C.; Mollah, Y. A. *Org. Mass Spectrom.* **1982**, *17*, 127–130.
32. Bombach, R.; Dannacher, J.; Honegger, E.; Stadelmann, J.-P.; Neier, R. *Chem. Phys.* **1983**, *82*, 459–470.
33. Bouchoux, G.; Flammang, R.; Maquestiau, A. *Org. Mass Spectrom.* **1985**, *20*, 154–155.
34. Borden, W. T., Ed. *Diradicals*; Wiley: New York, 1982.
35. Wentrup, C. *Reactive Molecules: The Neutral Reactive Intermediate in Organic Chemistry*; Wiley-Interscience: New York, 1984; pp 128–161.
36. Cordero, M. M.; Houser, J. J.; Wesdemiotis, C. *Anal. Chem.* **1993**, *65*, 1594–1601.
37. (a) Danis, P. O.; Feng, R.; McLafferty, F. W. *Anal. Chem.* **1985**, *58*, 348–354; (b) Hop, C. E. C. A.; Holmes, J. L. *Org. Mass Spectrom.* **1991**, *26*, 476–480.
38. Burgers, P. C.; Holmes, J. L.; Mommers, A. A.; Terlouw, J. K. *Chem. Phys. Lett.* **1983**, *102*, 1–3.
39. Cooks, R. G.; Beynon, J. H.; Caprioli, R. M.; Lester, G. R. *Metastable Ions*; Elsevier: Amsterdam, 1973.
40. Holmes, J. L. *Org. Mass Spectrom.* **1985**, *20*, 169–183.
41. (a) Magrane, J. K.; Cottle, D. L. *J. Am. Chem. Soc.* **1942**, *64*, 484–487; (b) Stahl, C. W.; Cottle, D. L. *J. Am. Chem. Soc.* **1943**, *65*, 1782–1783.
42. Roberts, J. D.; Chambers, V. C. *J. Am. Chem. Soc.* **1951**, *73*, 3176–3179.
43. Polce, M. J.; Wesdemiotis, C. *J. Am. Chem. Soc.* **1993**, *115*, 10849–10856.
44. Holmes, J. L.; Lossing, F. P. *J. Am. Chem. Soc.* **1980**, *102*, 1591 1595.
45. Levsen, K. *Fundamental Aspects of Organic Mass Spectrometry*; Verlag Chemie: Weinheim, 1978.
46. Bouchoux, G.; Hoppilliard, Y.; Flammang, R.; Maquestiau, A.; Meyrant, P. *Org. Mass Spectrom.* **1983**, *18*, 340–344.
47. Burgers, P. C.; Mommers, A. A.; Holmes, J. L. *J. Am. Chem. Soc.* **1983**, *105*, 5976–5979.

48. McLafferty, F. W.; Turecek, F. *Interpretation of Mass Spectra*, 4th ed.; University Science Books: Mill Valley, CA, 1993.
49. Kimura, K.; Katsumata, S.; Achiba, Y.; Yamazaki, T.; Iwata, S. *Handbook of Hel Photoelectron Spectra of Fundamental Organic Molecules*; Halsted Press: New York, 1981.
50. McAdoo, D. J. *Mass Spectrom. Rev.* **1988**, *7*, 363–393.
51. McAdoo, D. J.; Hudson, C. E.; Traeger, J. C. *Int. J. Mass Spectrom. Ion Processes* **1987**, *79*, 183–187.
52. (a) Lifshitz, C.; Tzidony, E. *Int. J. Mass Spectrom. Ion Phys.* **1981**, *39*, 181–195; (b) Turecek, F.; McLafferty, F. W. *J. Am. Chem. Soc.* **1984**, *106*, 2525–2528; (c) McAdoo, D. J.; Hudson, C. E. *Int. J. Mass Spectrom. Ion Processes* **1984**, *59*, 77–83.
53. (a) Turecek, F.; McLafferty, F. W. *J. Am. Chem. Soc.* **1984**, *106*, 2528–2531; (b) Lifshitz, C. *Org. Mass Spectrom.* **1988**, *23*, 303–306.
54. (a) Danis, P. O.; Wesdemiotis, C.; McLafferty, F. W. *J. Am. Chem. Soc.* **1983**, *105*, 7454–7456; (b) Terlouw, J. K.; Kieskamp, W. M.; Holmes, J. L.; Mommers, A. A.; Burgers, P. C. *Int. J. Mass Spectrom. Ion Processes* **1985**, *64*, 245–250.
55. Gilpin, J. A.; McLafferty, F. W. *Anal. Chem.* **1957**, *29*, 990–994.
56. Drewello, T.; Heinrich, N.; Maas, W. P. M.; Nibbering, N. M. M.; Weiske, T.; Schwarz, H. *J. Am. Chem. Soc.* **1987**, *109*, 4810–4818.
57. Goldberg, N.; Schwarz, H. *Acc. Chem. Res.* **1994**, *27*, 347–352.
58. Pedersen, S.; Herek, J. L.; Zewail, A. H. *Science* **1994**, *266*, 1359–1364.
59. Zagorevskii, D. V.; Holmes, J. L. *Mass Spectrom. Rev.* **1994**, *13*, 133–154.
60. Cohen, N.; Benson, S. W. *Chem. Rev.* **1993**, *93*, 2419–2438.